Enclosure 3
Supplement to Topical Report R003-03-002106
"Validation of B&W mPower Core Design Methods"
MPWR-TOPR-000001 (Redacted)

babcock & wilcox mPower

Supplement to Topical Report R003-03-002106
Validation of B&W mPower Core Design Methods
MPWR-TOPR-000001
Revision 000
August 2012

B&W mPower™
a progressive energy solution

B&W mPower™ Reactor Program
Babcock & Wilcox mPower, Inc.
109 Ramsey Place
Lynchburg, VA 24501

(Redacted Version)

© 2012 BABCOCK & WILCOX mPOWER, INC. ALL RIGHTS RESERVED.
This document is the property of Babcock & Wilcox mPower, Inc. (B&W mPower)

Document No.	Title	Rev. No.
MPWR-TOPR-000001	Validation of B&W mPower Core Design Methods	**000**

SIGNATURES			
Prepared By:	Dudley A. Raine, III	Dudley A. Raine, III	8/29/12
	Printed Name or Title	Signature	Date
Reviewed By:	Joshua J. Bergman	Josh Bergman	8/29/12
	Printed Name or Title	Signature	Date
Reviewed By:	Gary W. Neeley	Gary W. Neeley	8/29/12
	Printed Name or Title	Signature	Date
Approved By:	Vincent J. Bilovsky	[illegible]	8/29/12
	Printed Name or Title	Signature	Date
Approved By:	Michael T. Childerson	MT Childerson	8/30/2012
	Printed Name or Title	Signature	Date

©2012 Babcock & Wilcox mPower, Inc. All rights reserved.

Document No.	Title	Rev. No.
MPWR-TOPR-000001	Validation of B&W mPower Core Design Methods	**000**

RECORD OF REVISION

Revision No.	Date	Preparer	Description of Changes
000	8/30/12	Dudley A Raine, III	Initial Issue

©2012 Babcock & Wilcox mPower, Inc. All rights reserved.

Executive Summary

The fundamental applicability and accuracy of the nuclear computational methodology that will be used in performing nuclear design calculations for the B&W mPower™ reactor core has been analyzed using an equivalent methodology developed for use with the Monte Carlo radiation transport code, ***MCNPX***. This work was performed primarily to respond to NRC questions and comments regarding the original topical submission Report R003-03-002106, Core Nuclear Design Codes and Methods Qualification, submitted to the NRC on August 31, 2010. Those questions and comments were related to the adequacy of the Studsvik Scandpower Core Management System (***CMS***) codes and methods to model small reactor cores that are more sensitive to their reflector configuration than existing large power reactors. Specific areas that are analyzed and compared include criticality conditions, nodal flux and power distributions, reactivity coefficients, control rod worths, and a core follow analysis. This report is intended to present a validation of the nuclear physics underlying the ***CMS*** codes and computational methodology that will be used when performing nuclear design calculations for the Babcock & Wilcox mPower™ reactor core.

This report describes a baseline B&W mPower core design and the analyses performed to characterize the design using the ***CMS*** code suite, which consists of the two-dimensional lattice physics and cross-section generation code ***CASMO-5***, the cross-section processing and functionalization code ***CMS-LINK***, and the three-dimensional core simulator, ***SIMULATE-3***. The ***CMS*** code suite is an industry standard, state-of-the-art computer code package for comprehensive neutronic simulation of light water reactors. The primary applications of the ***CMS*** code package include fuel bundle design (e.g., enrichment zoning and burnable poison design), incore fuel management and loading pattern optimization, evaluation of fuel cycle energy, and various fuel and core licensing calculations (e.g., reactivity coefficients and shutdown margin). A complete discussion of the B&W mPower reference design used for this report as developed using the ***CMS*** code suite is presented herein.

Validation of the ***CMS*** computational methodology and the underlying physics is accomplished using ***MCNPX***, Version 2.7.0. A model of the B&W mPower reactor core was constructed for use with ***MCNPX*** and was designed with the same radial and homogenized upper and lower reflector materials and dimensions as those used in the ***SIMULATE-3*** analyses. Nodal temperature and density data for the fuel, cladding, and moderator from the output of the ***SIMULATE-3*** design calculations were used as inputs in ***MCNPX*** to ensure that the material properties between the two models were consistent for all calculations. Depletion calculations were performed with ***MCNPX*** and compared against both ***CASMO-5*** lattice depletions and the ***SIMULATE-3*** core operational cycle.

The results of these analyses show that the methods used in the ***CMS*** suite are fully capable of modeling a small reactor core like the B&W mPower design.

Lattice comparisons and ***MCNPX*** and ***CASMO-5*** were performed and all results showed excellent agreement. The variations in k-infinity for BOC lattices under cold and hot conditions were all less than [ ] The lattice depletions runs performed in ***CASMO-5*** and ***MCNPX*** also compared very well with BOC differences less than [

]

©2012 Babcock & Wilcox mPower, Inc. All rights reserved.

Similarly, the flux and current values in the analyses of the reflector performed with ***CASMO-5*** and ***MCNPX*** show a high degree of consistency with minor differences shown in regions close to the core boundary. The differences [

]

Comparisons were performed between ***SIMULATE-3*** and ***MCNPX*** with equivalent, full core nodalized models. Startup physics calculations and depletion analyses were conducted. The comparisons of various core configurations at BOC showed excellent agreement, with the greatest differences noted at highly subcritical conditions where the Monte Carlo method for calculating criticality is questionable. The depletion analyses were also highly consistent between the two codes, with mean differences generally less than [ ] Further, the thermal and fast flux profiles were very similar, even being able to distinguish the placement of the midgrids in many of the assemblies in the profile produced by both ***MCNPX*** and ***SIMULATE-3***.

Based on the results, the ***CMS*** suite and methodologies are judged to be fully validated and qualified to perform design calculations and analyses for the B&W mPower reactor.

©2012 Babcock & Wilcox mPower, Inc. All rights reserved.

TABLE OF CONTENTS

1. INTRODUCTION 12
2. BACKGROUND 13
- 2.1 General Information 13
- 2.2 Assembly Design Details 14
- 2.3 Core Design Summary 19
- 2.4 Code Summary 20

3. METHODOLOGY 21
- 3.1 Lattice Construction 21
- 3.2 Design Specification 24
- 3.3 Lattice Modeling Considerations 24
- 3.4 Cross Section and Energy Considerations 26
- 3.5 Full Core Benchmark Comparison Methods 29
- 3.6 Reflector Calculations 31
- 3.7 Reflector Calculational Methodology 35
- 3.8 Reflector Modeling Considerations 38

4. *SIMULATE-3* REFERENCE CORE OPERATING CYCLE 40
- 4.1 Design Specifications 40
- 4.2 Cycle Management (Control Rod Patterns) 42
- 4.3 ***SIMULATE-3*** Results 44

5. RESULTS, COMPARISON and ANALYSIS 51
- 5.1 Lattice Results 51
- 5.2 Reflector Results 55
- 5.3 Startup Physics Calculation Comparisons 78
- 5.4 ***SIMULATE-3/MCNPX*** Core Depletion Comparison 80

6. SUMMARY and CONCLUSIONS 107
- 6.1 Results Summary 107
- 6.2 Conclusions 108

7. List of Acronyms 110
8. REFERENCES 112

Appendix A Additional Background Details 113
Appendix B Additional Methodology Details 127
Appendix C Additional Details of the *SIMULATE-3* Reference Core Operating Cycle 151
Appendix D Additional Details of Results, Comparison, and Analysis 169

©2012 Babcock & Wilcox mPower, Inc. All rights reserved.

List of Figures

Figure 1. Core Former and Fuel Assemblies with Control Rod Spiders 13
Figure 2. Basic Lattice Configuration 15
Figure 3. Lattice Layout for Assemblies with [ ] 16
Figure 4. Lattice Layout for Assemblies with [ ] 16
Figure 5. Lattice Layout for Assemblies with [ ] 17
Figure 6. B&W mPower Fuel Lattice Nomenclature 18
Figure 7. Comparison of Lattice Depletion K-Infinity Values [ ] 23
Figure 8. Differences in K-infinity Values as a Function of Burnup Between the Two *MCNPX* Lattice Models 23
Figure 9. Histogram Showing the Distribution of the Differences of the K-Infinity Values Between the Two *MCNPX* Lattice Models 24
Figure 10. Comparison of *CASMO-5* K-Infinity Values With and Without Resonance Upscattering Correction 26
Figure 11. Comparison of Depletion of [ ] 27
Figure 12. Comparison of Depletion of [ ] 27
Figure 13. Comparison of Depletion of [ ] 28
Figure 14. Comparison of Depletion of [ ] 29
Figure 15. Cross Section of Upper Reflector Concept Design 32
Figure 16. Cross Section View of Lower Reflector Concept Design 33
Figure 17. Cross Section of Radial Reflector Concept Design 33
Figure 18. Cross Section View of Homogenized Upper Axial Reflector 34
Figure 19. Cross Section View of Homogenized Lower Axial Reflector 35
Figure 20. Cross Section View of Radial Reflector 35
Figure 21. mPower Fuel Assembly Summary 41
Figure 22. mPower Fuel Type Core Map 42
Figure 23. Summary of Control Rod Patterns used from BOC to [ ] 43
Figure 24. Power Axial Offset versus Cycle Exposure 45
Figure 25. Nodal Peaking versus Cycle Exposure 46
Figure 26. Hot Excess Reactivity versus Cycle Exposure 46
Figure 27. Axial Power Profile at BOC 47
Figure 28. Axial Power Profile [ ] 48
Figure 29. Axial Power Profile [ ] 49
Figure 30. Axial Power Profile [ ] 50
Figure 31. Comparison of *CASMO-5* and *MCNPX* Depletion [ ] 53
Figure 32. Comparison of *CASMO-5* and *MCNPX* Depletion [ ] 54
Figure 33. Comparison of *CASMO-5* and *MCNPX* Depletion [ ] 54
Figure 34. Homogenized Upper Reflector Detail 56
Figure 35. Homogenized Lower Reflector Detail 56

©2012 Babcock & Wilcox mPower, Inc. All rights reserved.

Figure 36. Radial Reflector Configuration [ ] 56
Figure 37. Net Current Profile in Upper Reflector for Energy Range 1 - 20 MeV 57
Figure 38. Net Current Profile in Upper Reflector for Energy Range 5.53 keV - 1 MeV 58
Figure 39. Net Current Profile in Upper Reflector for Energy Range 0.625 eV - 5.53 keV 58
Figure 40. Net Current Profile in Upper Reflector for Energy Range <0.625 eV 59
Figure 41a. Flux profile in Upper Reflector for Energy Range 1 - 20 MeV 60
Figure 41b. Flux profile in Upper Reflector for Energy Range 1 - 20 MeV (Log Scale) 60
Figure 42a. Flux Profile in Upper Reflector for Energy Range 5.53 keV - 1 MeV 61
Figure 42b. Flux Profile in Upper Reflector for Energy Range 5.53 keV - 1 MeV (Log Scale) 61
Figure 43a. Flux Profile in Upper Reflector for Energy Range 0.625 eV - 5.53 keV 62
Figure 43b. Flux Profile in Upper Reflector for Energy Range 0.625 eV - 5.53 keV (Log Scale) 62
Figure 44a. Flux Profile in Upper Reflector for Energy Range <0.625 eV 63
Figure 44b. Flux Profile in Upper Reflector for Energy Range <0.625 eV (Log Scale) 63
Figure 45. Net Current Profile in Lower Reflector for Energy Range 1 - 20 MeV 64
Figure 46. Net Current Profile in Lower Reflector for Energy Range 5.53 keV - 1 MeV 65
Figure 47. Net Current Profile in Lower Reflector for Energy Range 0.625 eV - 5.53 keV 65
Figure 48. Net Current Profile in Lower Reflector for Energy Range <0.625 eV 66
Figure 49a. Flux profile in Lower Reflector for Energy Range 1 - 20 MeV 67
Figure 49b. Flux profile in Lower Reflector for Energy Range 1 - 20 MeV (Log Scale) 67
Figure 50a. Flux Profile in Lower Reflector for Energy Range 5.53 keV - 1 MeV 68
Figure 50b. Flux Profile in Lower Reflector for Energy Range 5.53 keV - 1 MeV (Log Scale) 68
Figure 51a. Flux Profile in Lower Reflector for Energy Range 0.625 eV - 5.53 keV 69
Figure 51b. Flux Profile in Lower Reflector for Energy Range 0.625 eV - 5.53 keV (Log Scale) 69
Figure 52a. Flux Profile in Lower Reflector for Energy Range <0.625 eV 70
Figure 52b. Flux Profile in Lower Reflector for Energy Range <0.625 eV (Log Scale) 70
Figure 53. Net Current Profile in Radial Reflector for Energy Range 1 - 20 MeV 71
Figure 54. Net Current Profile in Radial Reflector for Energy Range 5.53 keV - 1 MeV 72
Figure 55. Net Current Profile in Radial Reflector for Energy Range 0.625 eV - 5.53 keV 72
Figure 56. Net Current Profile in Radial Reflector for Energy Range <0.625 eV 73
Figure 57a. Flux profile in Radial Reflector for Energy Range 1 - 20 MeV 74
Figure 57b. Flux profile in Radial Reflector for Energy Range 1 - 20 MeV (Log Scale) 74
Figure 58a. Flux Profile in Radial Reflector for Energy Range 5.53 keV - 1 MeV 75
Figure 58b. Flux Profile in Radial Reflector for Energy Range 5.53 keV - 1 MeV (Log Scale) 75
Figure 59a. Flux Profile in Radial Reflector for Energy Range 0.625 eV - 5.53 keV 76
Figure 59b. Flux Profile in Radial Reflector for Energy Range 0.625 eV - 5.53 keV (Log Scale) 76
Figure 60a. Flux Profile in Radial Reflector for Energy Range <0.625 eV 77
Figure 60b. Flux Profile in Radial Reflector for Energy Range <0.625 eV (Log Scale) 77
Figure 61. Quarter Core Control Rod Group Map (Mirror Symmetric) 81
Figure 62a. K-effective as a Function of Burnup 83
Figure 62b. K-effective as a Function of Burnup (Log Scale) 83
Figure 63a. Difference in K-effective Values Between *MCNPX* and *SIMULATE-3* 84
Figure 63b. Difference in K-effective Values Between *MCNPX* and *SIMULATE-3* (Log Scale) 84
Figure 64a. All Rods Out K-effective Comparison 85
Figure 64b. All Rods Out K-effective Comparison (Log Scale) 85
Figure 65a. Difference in ARO K-effective Values Between MCNPX and SIMULATE-3 86

©2012 Babcock & Wilcox mPower, Inc. All rights reserved.

Figure 65b. Difference in ARO K-effective Values Between MCNPX and SIMULATE-3 (Log Scale) 86
Figure 66. Assembly Relative Power Fraction Profiles at BOC, Critical Hot Full Power 87
Figure 67. Assembly Thermal Flux Profiles at BOC, Critical Hot Full Power 88
Figure 68. Assembly Fast Flux Profiles at BOC, Critical Hot Full Power 89
Figure 69. Assembly Relative Power Fraction Profiles at [ ] 90
Figure 70. Assembly Thermal Flux Profiles at [ ] 91
Figure 71. Assembly Fast Flux Profiles at [ ] 92
Figure 72. Assembly Relative Power Fraction Profiles at [ ] 93
Figure 73. Assembly Thermal Flux Profiles at [ ] 94
Figure 74. Assembly Fast Flux Profiles at [ ] 95
Figure 75. Assembly Relative Power Fraction Profiles at BOC, All Rods Out Hot Full Power 96
Figure 76. Assembly Thermal Flux Profiles at BOC, All Rods Out Hot Full Power 97
Figure 77. Assembly Fast Flux Profiles at BOC, All Rods Out Hot Full Power 98
Figure 78. Assembly Relative Power Fraction Profiles at [ ] All Rods Out Hot Full Power 99
Figure 79. Assembly Thermal Flux Profiles at [ ] All Rods Out Hot Full Power 100
Figure 80. Assembly Fast Flux Profiles at [ ] All Rods Out Hot Full Power 101
Figure 81. Assembly Relative Power Fraction Profiles at [ ] All Rods Out Hot Full Power 102
Figure 82. Assembly Thermal Flux Profiles at [ ] All Rods Out Hot Full Power 103
Figure 83. Assembly Fast Flux Profiles at [ ] All Rods Out Hot Full Power 104
Figure 84. Histogram of Difference Distribution at BOC, [ ] (from left to right) 105
Figure 85. Assembly Average and Maximum Relative Power Fractions at BOC, [ ] 106

Figure A - 1. *INTERPIN-4* Program Flow 114
Figure A - 2. *CASMO-5* Program Computational Flow 117
Figure A - 3. Axial Cross Section View of *SIMULATE-3*-Equivalent *MCNPX* Model 124
Figure A - 4. Radial Cross Section View of *SIMULATE-3*-Equivalent *MCNPX* Model 125

Figure B - 1. *CASMO-5* Title and Name Card Input 141
Figure B - 2. *CASMO-5* Global Operating Parameters 142
Figure B - 3. *CASMO-5* Material Specifications 142
Figure B - 4. *CASMO-5* Pin Geometry Specifications 143
Figure B - 5. *CASMO-5* Fuel and Pin Array Specifications 144
Figure B - 6. Closing *CASMO-5* Input Cards 144
Figure B - 7. *CASMO-5* Input Card Image For Homogenized Upper Reflector 148
Figure B - 8. *CASMO-5* Input Card Image For Homogenized Lower Reflector 150

Figure C - 1. The [ ] Used in the mPower Cycle Management 152
Figure C - 2. The [ ] Used in the mPower Cycle Management 153
Figure C - 3. Summary of Control Rod Patterns Used from BOC to EOC 155

©2012 Babcock & Wilcox mPower, Inc. All rights reserved.

Figure C - 4. Power Axial Offset versus Cycle Exposure 162
Figure C - 5. Nodal Peaking versus Cycle Exposure 163
Figure C - 6. Cold Shutdown Margin versus Cycle Exposure 164
Figure C - 7. Hot Excess Reactivity versus Cycle Exposure 165
Figure C - 8. Control Rod Movement versus Cycle Exposure 166
Figure C - 9. End of Full Power [ ] Axial Power Profile 167
Figure C - 10. End of Full Power [ ] Exposure Profile 168

Figure D - 1. Comparison of *CASMO-5* and *MCNPX* Depletion for [ ]..... 169
Figure D - 2. Comparison of *CASMO-5* and *MCNPX* Depletion [ ]..... 170
Figure D - 3. Comparison of *CASMO-5* and *MCNPX* Depletion [ ]..... 170
Figure D - 4. Comparison of *CASMO-5* and *MCNPX* Depletion [ ]..... 171
Figure D - 5. Comparison of *CASMO-5* and *MCNPX* Depletion [ ]..... 171
Figure D - 6. Comparison of *CASMO-5* and *MCNPX* Depletion [ ]..... 172
Figure D - 7. Comparison of *CASMO-5* and *MCNPX* Depletion[ ]..... 172
Figure D - 8. Comparison of *CASMO-5* and *MCNPX* Depletion[ ]..... 173

©2012 Babcock & Wilcox mPower, Inc. All rights reserved.

List of Tables

Table 1. Homogenization Fractions for the Upper Reflector 36
Table 2. Homogenization Fractions for the Lower Reflector 37
Table 3. Radial Reflector Slabs 38
Table 4. mPower Cycle Energy and Key Results Summary 40
Table 5. mPower Fuel Assembly Average U-235 Enrichments 41
Table 6. Comparison of Un-rodded Lattice K-infinity Values at Cold Conditions, BOC 51
Table 7. Comparison of Rodded Lattice K-infinity Values at Cold Conditions, BOC 52
Table 8. Comparison of Un-rodded Lattice K-infinity Values at Hot Conditions, BOC 52
Table 9. Comparison of Rodded Lattice K-infinity Values at Hot Conditions, BOC 53
Table 10. Comparison of K-Effective Values at Several BOC Configurations using MCNPX and SIMULATE-3 78
Table 11. Data for SIMULATE-3 and MCNPX Core Depletion Simulations 82

Table A - 1. *INTERPIN-4* Input Parameters 121

Table B - 1. B&W mPower *CASMO-5* Control Rod Assembly Specification 130
Table B - 2. Fuel Assembly Mechanical Design Inputs 130
Table B - 3. Neutronic Design Parameters 131
Table B - 4. B&W mPower Operating Characteristics 141

©2012 Babcock & Wilcox mPower, Inc. All rights reserved.

1. INTRODUCTION

This report presents a validation of the physics underlying the codes and nuclear computational methodology that will be used in performing nuclear design calculations for the Babcock & Wilcox mPower™ reactor core. The analyses herein are a supplement to Report R003-03-002106, "Core Nuclear Design Codes and Methods Qualification" [Reference 1], submitted August 31, 2010. That report presented an analysis of Cycles 1 and 2 of Three Mile Island (TMI), Unit 1, and various critical experiments using the Studsvik Scandpower Core Management System (***CMS***).

This report demonstrates that the applicability of the ***CMS*** code suite is not limited to large reactor core designs and that the suite may also be used to model small cores like that of the B&W mPower reactor. Since there are no other reactors similar in size, shape, and type, and with publicly available operational data against which the ***CMS*** codes can be validated, an alternative benchmark was developed and is herein presented and analyzed. The applicability of the ***CMS*** code suite to a small core design is shown through the establishment of a comprehensive first principles benchmark model that is fully capable of replicating the detailed physics of such a core. The benchmark model is used to demonstrate the ability of the ***CMS*** suite to adequately model the leakage, the spectrum and magnitude of the concomitant reflected neutrons, and their effect on the overall operating characteristics of the core.

The benchmark is a full scale model of the B&W mPower reactor core developed for and analyzed in the radiation transport code Monte Carlo N-Particle eXtended ***(MCNPX***) Version 2.7.0, a first principles physics code capable of modeling all of the detailed structures in a typical core design and the subsequent transport of neutrons through those structures. Version 2.7.0 of the code, developed and maintained by Los Alamos National Laboratory (LANL) [Reference 2], from here on will be referred to as ***MCNPX***, includes ***CINDER90***, a LANL code that performs isotope generation and depletion calculations. ***CINDER90*** performs the "depletion" of user-selected materials in the model during criticality runs, simulating the operational buildup of fission products from fission of the fuel in an operating reactor and concomitant transformation of those fission products and other user-specified materials through neutron capture and radioactive decay. The released ***MCNPX*** package also includes a complete set of ENDF/B-VII cross sections processed at various temperatures to account for Doppler broadening.

Unlike the ***CMS*** code suite, ***MCNPX*** does not have a reactor simulator module. The area where ***MCNPX*** excels is in the detailed calculation of the transport of radiation through Monte Carlo methods using explicit energy-dependent microscopic cross sections. Thus, there is no capability in ***MCNPX*** to calculate the effect of the thermal feedback of the moderator on the core as a whole for any given operating point, and using ***MCNPX*** in an actual design mode is not possible with current computational technology. However, by incorporating consistent design features (e.g., thermal expansion and material compositions) from ***CASMO-5*** [Reference 3] and copying a limited set of the nodal characteristics (e.g., fuel, clad, and moderator temperatures and densities) from ***SIMULATE-3*** [Reference 4] for a given statepoint, ***MCNPX*** can be used to mimic the operation of ***SIMULATE-3*** with all the detailed physics and cross sections of a Monte Carlo transport code. With ***MCNPX***, it is possible to construct a model of the B&W mPower core and perform a comparative core follow that, along with the results of the original topical report submission validates the use of the ***CMS*** codes and methodology for the B&W mPower Reference Core Design.

©2012 Babcock & Wilcox mPower, Inc. All rights reserved.

2. BACKGROUND

2.1 General Information

The B&W mPower Reactor concept design is a passively safe, pressurized water reactor with the steam generator, pressurizer, and control rod drives internal to the pressure vessel. The reactor is designed for a power output of 530 MWt. The reactor core consists of 69 mechanically identical fuel assemblies arranged in a pattern which approximates a right circular cylinder. The fuel assemblies are surrounded by a solid stainless steel core former (see Figure 1). The reactor is designed for a one batch, four year operating cycle between refueling and a total design life of 60 years.

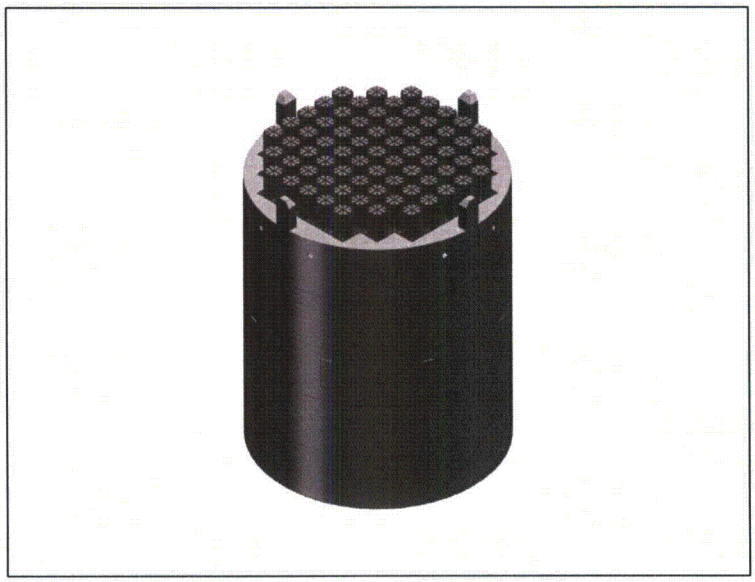

Figure 1. Core Former and Fuel Assemblies with Control Rod Spiders

The B&W mPower reactor does not use soluble boron poison (chemical shim) during normal operation, and reactivity control is provided by 69 full-length control rod assemblies (CRAs), which are located in guide tubes within the fuel assemblies, and both lumped and integral fuel burnable absorbers. The CRAs primarily consist of 24 control rodlets, but [

]

©2012 Babcock & Wilcox mPower, Inc. All rights reserved.

[

]

Because the B&W mPower core is designed for a one batch extended cycle operation, [

]

2.2 Assembly Design Details

2.2.1 Lattice Configuration

The B&W mPower fuel assembly is based on a standard 17x17 PWR pin array on a [

]

©2012 Babcock & Wilcox mPower, Inc. All rights reserved.

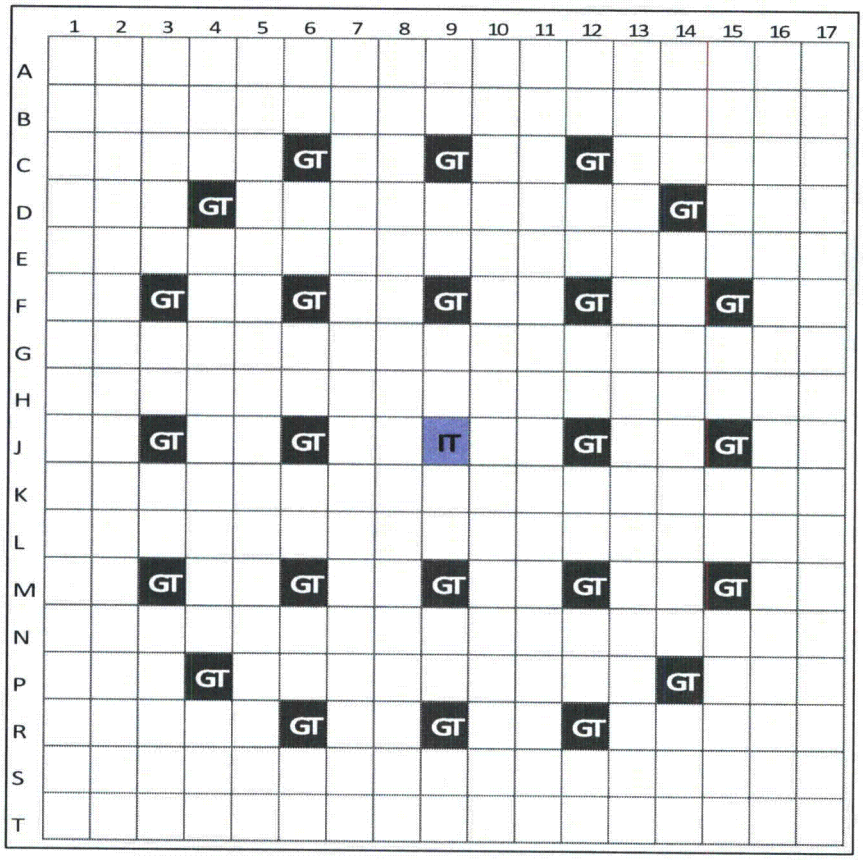

Figure 2. Basic Lattice Configuration

[

]

©2012 Babcock & Wilcox mPower, Inc. All rights reserved.

[

]

Figure 3. Lattice Layout for Assemblies with [ ]

[

]

Figure 4. Lattice Layout for Assemblies with [ ]

©2012 Babcock & Wilcox mPower, Inc. All rights reserved.

[

]

Figure 5. Lattice Layout for Assemblies with [ ]

2.2.2 Lattice Nomenclature

[

]

©2012 Babcock & Wilcox mPower, Inc. All rights reserved.

[

]

Figure 6. B&W mPower Fuel Lattice Nomenclature

[

]

[

]

©2012 Babcock & Wilcox mPower, Inc. All rights reserved.

2.2.3 Reflector Configuration

[

]

2.3 Core Design Summary

The reference design configuration described and analyzed herein is based on a frozen representative design as of January 11, 2012. A few minor changes have been made to the operating conditions (pressure, inlet and outlet temperatures, and mass flow rate) of the reactor since that time, but the fundamental configuration of the core itself has remained the same. There are five different bundle types distributed among the 69 bundle locations in the B&W mPower core. [

] At the end of each cycle, all 69 fuel assemblies are replaced with fresh fuel. Thus, each fresh core must carry sufficient U-235 (at less than 5 percent enrichment) within its 69 fuel assemblies to run for that amount of time while maintaining a low excess reactivity that guarantees the core can be safely shut down using the available control rods and allowing for operation well within appropriate limits for power distribution and peaking.

[

]

The operating conditions for the mPower reference design are determined based on the thermal power output, a heat balance between the primary and secondary sides of the integral steam generator, and the requirements necessary to drive the turbine. Based on an analysis of the aforementioned overall system parameters and requirements, inlet and outlet temperatures of 564 °F and 608 °F, respectively, at a nominal flow rate of 30.0 Mlb-m/hr, combined with a feed-water temperature of 414 °F at 825 psi provide the necessary 50 °F of superheat on the secondary side to drive the turbine system. The nominal operating pressure in the pressurizer is 2050 psi, which translates to approximately 2070 psi at the core midplane. These parameters form the basis for the initial core design process.

©2012 Babcock & Wilcox mPower, Inc. All rights reserved.

2.4 Code Summary

The Studsvik Scandpower ***CMS*** Code Suite and LANL ***MCNPX*** were used to construct models of the mPower core. The following provides a brief summary of each code; more detailed descriptions are found in Appendix A.

2.4.1 ***CMS*** Code Suite

The ***CMS*** Code Suite comprises two primary codes ***CASMO-5/SIMULATE-3*** and two supporting codes ***INTERPIN-4/CMS-LINK***. ***CASMO-5*** is a multigroup, two-dimensional transport theory code used to generate lattice cross sections for ***SIMULATE-3***, which is a three dimensional, two-group, steady-state reactor core simulator used to perform incore fuel management studies, core design calculations, and calculations of reactor safety parameters. ***INTERPIN-4*** [Reference 5] calculates the steady-state fuel temperature behavior of UO_2 fuel in light water reactor cores. It is used to provide best estimate fuel temperature data for ***CASMO-5*** and ***SIMULATE-3***. ***CMS-LINK*** [Reference 6] is a linking code that processes cross section files produced by ***CASMO-5*** into a binary formatted library that can be used by ***SIMULATE-3***.

2.4.2 ***MCNPX***

MCNPX is a first principles, three-dimensional Monte Carlo radiation transport code developed and maintained by Los Alamos National Laboratory. The current version of ***MCNPX***, Version 2.7.0, was released by LANL through the Radiation Safety Information and Computational Center (RSICC) in July 2011. ***MCNPX*** uses continuous energy cross section libraries based on ENDF/B-VII, and uses the ***CINDER90*** code for isotopic depletion in conjunction with kcode criticality calculations.

©2012 Babcock & Wilcox mPower, Inc. All rights reserved.

3. METHODOLOGY

3.1 Lattice Construction

3.1.1 ***CASMO-5*** Lattice Construction

The construction of the lattices for ***CASMO-5*** [Reference 3] is a reasonably straightforward process. The input requires basic information, including the average fuel and moderator temperatures obtained from ***INTERPIN-4*** [Reference 5]. [

]

3.1.2 ***MCNPX*** Lattice Construction

[

]

[ ]

©2012 Babcock & Wilcox mPower, Inc. All rights reserved.

[

]

3.1.3 ***MCNPX*** Lattice Depletion Simulations

[

]

©2012 Babcock & Wilcox mPower, Inc. All rights reserved.

[

]

Figure 7. Comparison of Lattice Depletion K-Infinity Values [

]

[

]

Figure 8. Differences in K-infinity Values as a Function of Burnup Between the Two *MCNPX* Lattice Models

©2012 Babcock & Wilcox mPower, Inc. All rights reserved.

[

]

Figure 9. Histogram Showing the Distribution of the Differences of the K-Infinity Values Between the Two *MCNPX* Lattice Models

3.2 Design Specification

A summary of the overall design specifications including mechanical design, mechanical arrangement and characteristics of the B&W mPower fuel assembly used in ***CASMO-5*** is presented in Appendix B § B.2.1. Also included in the Appendix are the Material Properties including the assumptions used for ***CMS*** code suite, the core operating parameters, and the lattice input specifications for ***CASMO-5.***

3.3 Lattice Modeling Considerations

3.3.1 *CASMO-5*

[

]

©2012 Babcock & Wilcox mPower, Inc. All rights reserved.

[

]

3.3.2 ***MCNPX***

[

]

3.3.3 Thermal Expansion

[

]

3.3.4 Boundary Conditions

The boundary conditions for standard ***CASMO-5*** lattice calculations, by default, are reflective. This effect is accomplished in ***MCNPX*** with a flag for each of the reflective surfaces in the input file.

3.3.5 Grid Effects

[

]

©2012 Babcock & Wilcox mPower, Inc. All rights reserved.

[

]

3.4 Cross Section and Energy Considerations

3.4.1 Resonance Upscattering

[

]

Figure 10. Comparison of *CASMO-5* K-Infinity Values With and Without Resonance Upscattering Correction

3.4.2 Uniform Quadrature

[

]

©2012 Babcock & Wilcox mPower, Inc. All rights reserved.

[

]

Figure 11. Comparison of Depletion of [

]

[

]

Figure 12. Comparison of Depletion of [

]

©2012 Babcock & Wilcox mPower, Inc. All rights reserved.

3.4.3 Energy Group Structure

[

]

]

Figure 13. Comparison of Depletion of [

]

©2012 Babcock & Wilcox mPower, Inc. All rights reserved.

[

]

Figure 14. Comparison of Depletion of [

]

[

]

3.5 Full Core Benchmark Comparison Methods

3.5.1 ***SIMULATE-3*** Core Design

The core design is accomplished with ***SIMULATE-3.*** [

]

©2012 Babcock & Wilcox mPower, Inc. All rights reserved.

3.5.2 ***SIMULATE-3/MCNPX*** Comparison Method

MCNPX does not have the capability to model dynamic changes in a complete reactor system in the same manner as ***SIMULATE-3***. [

]

©2012 Babcock & Wilcox mPower, Inc. All rights reserved.

[

]

3.6 Reflector Calculations

3.6.1 Reflector Configuration

The reflectors comprise the regions just outside the boundaries of the active core.
[

]

©2012 Babcock & Wilcox mPower, Inc. All rights reserved.

[

]

Figure 15. Cross Section of Upper Reflector Concept Design

©2012 Babcock & Wilcox mPower, Inc. All rights reserved.

[

]

Figure 16. Cross Section View of Lower Reflector Concept Design

[

]

Figure 17. Cross Section of Radial Reflector Concept Design

©2012 Babcock & Wilcox mPower, Inc. All rights reserved.

[

]

[

]

Figure 18. Cross Section View of Homogenized Upper Axial Reflector

©2012 Babcock & Wilcox mPower, Inc. All rights reserved.

[

]

Figure 19. Cross Section View of Homogenized Lower Axial Reflector

[

]

Figure 20. Cross Section View of Radial Reflector

3.7 Reflector Calculational Methodology

3.7.1 Homogenized Reflector Description

Reference 3, as well as supplementary Studsvik training materials, state that the reflector slab material specification should use homogenized materials, which may be composed of various default compositions or user input specified compositions. [

]

©2012 Babcock & Wilcox mPower, Inc. All rights reserved.

[

]

3.7.2 Upper Reflector

The upper reflector was divided [

]

Table 1. Homogenization Fractions for the Upper Reflector

[

]

©2012 Babcock & Wilcox mPower, Inc. All rights reserved.

3.7.3 Lower Reflector

The lower reflector was divided [

]

Table 2. Homogenization Fractions for the Lower Reflector

[

]

©2012 Babcock & Wilcox mPower, Inc. All rights reserved.

3.7.4 Radial Reflector

The radial reflector was [

]

Table 3. Radial Reflector Slabs

[

]

3.8 Reflector Modeling Considerations

3.8.1 ***CASMO-5***

Reflector calculations are performed in ***CASMO-5*** in a different manner from standard lattice calculations. [

]

©2012 Babcock & Wilcox mPower, Inc. All rights reserved.

[

]

3.8.2 ***MCNPX***

Adapting the ***MCNPX*** lattices to perform a reflector calculation equivalent to that in ***CASMO-5*** is a straightforward process. [

]

3.8.3 Thermal Expansion

[

]

©2012 Babcock & Wilcox mPower, Inc. All rights reserved.

4. *SIMULATE-3* REFERENCE CORE OPERATING CYCLE

This core design concept utilizes a number of different lattice designs, with varying burnable poison content and pellet enrichment, and [

]

Table 4. mPower Cycle Energy and Key Results Summary

[

]

4.1 Design Specifications

The mPower core loading includes [

]

©2012 Babcock & Wilcox mPower, Inc. All rights reserved.

[

]

[

]

Figure 21. mPower Fuel Assembly Summary

Table 5. mPower Fuel Assembly Average U-235 Enrichments

[

]

©2012 Babcock & Wilcox mPower, Inc. All rights reserved.

[

]

Figure 22. mPower Fuel Type Core Map

4.2 Cycle Management (Control Rod Patterns)

This section summarizes the control rod sequences (see Figure 23) used from BOC to [ ] to control the excess reactivity of the core and to shape the axial and radial power and exposure distribution. The control rod sequences and location assignments within the assembly are provided in the Appendix C § C.1.1. [

]

©2012 Babcock & Wilcox mPower, Inc. All rights reserved.

[

]

Figure 23. Summary of Control Rod Patterns used from BOC to [ ]

©2012 Babcock & Wilcox mPower, Inc. All rights reserved.

[

]

Figure 23. Summary of Control Rod Patterns used from BOC to [ ]

[

]

4.3 ***SIMULATE-3*** Results

The ***SIMULATE-3*** results in this section of the report are given for the range from [

]

Comparable data were also generated using the results of the simulation with ***MCNPX***. Those results and a comparison with the ***SIMULATE-3*** results are presented in Section 5

4.3.1 BOC Shutdown Margin

At BOC, the measured cold shutdown margin (CSDM) as compared to the predicted CSDM calculated by ***SIMULATE-3*** is a very important element of the Physics Startup Test Program. [

]

4.3.2 Core Axial Offset

Axial offset is defined as the percent difference between the power generated in the upper and the lower halves of the core:

$$\text{Axial Offset} = (Pt - Pb) / (Pt + Pb) \times 100,$$

©2012 Babcock & Wilcox mPower, Inc. All rights reserved.

where Pt and Pb are the integrated powers (sum of nodal powers, as calculated in ***SIMULATE-3***) in the top and bottom halves of the core, respectively.

SIMULATE-3 lists the axial offset values as A-O = (Pt – Pb) / (Pt + Pb), as shown in Figure 24.

[

]

Figure 24. Power Axial Offset versus Cycle Exposure

4.3.3 Nodal Peaking

Nodal peaking values, as shown in Figure 25, represent the peak relative power density at a given exposure. [

]

©2012 Babcock & Wilcox mPower, Inc. All rights reserved.

[

]

Figure 25. Nodal Peaking versus Cycle Exposure

4.3.4 Hot Excess Reactivity

The hot excess reactivity (HExR), as shown in Figure 26, is the amount of reactivity that must be controlled at normal full power operating conditions using control rods. Hot excess reactivity is defined as the amount of reactivity, expressed in %Δk/k, by which the reactor would exceed criticality if all CRAs were withdrawn at rated conditions. The higher the hot excess reactivity, the greater the control rod density needed to maintain the reactor at the full power critical state. HExR is calculated with ***SIMULATE-3*** by running all rods out (ARO) cases, at rated conditions, restarting from the desired statepoints (exposures) in the nominal cycle run. Unlike the cold shutdown margin, hot excess reactivity is a core-wide phenomenon.

[

]

Figure 26. Hot Excess Reactivity versus Cycle Exposure

©2012 Babcock & Wilcox mPower, Inc. All rights reserved.

4.3.5 Bundle Power Profile at [ ]

[

]

[

]

Figure 27. Axial Power Profile at BOC

©2012 Babcock & Wilcox mPower, Inc. All rights reserved.

[

]

Figure 28. Axial Power Profile [ ]

©2012 Babcock & Wilcox mPower, Inc. All rights reserved.

[

]

Figure 29. Axial Power Profile [ ]

©2012 Babcock & Wilcox mPower, Inc. All rights reserved.

[

]

Figure 30. Axial Power Profile [ ]

©2012 Babcock & Wilcox mPower, Inc. All rights reserved.

5. RESULTS, COMPARISON and ANALYSIS

5.1 Lattice Results

5.1.1 ***CASMO-5/MCNPX*** Lattice Comparisons at BOC

The only parameter of particular relevance in comparing ***CASMO-5*** and ***MCNPX*** lattice depletions is the [

]

5.1.1.1 Comparisons at Cold Conditions

The first lattice comparisons between ***MCNPX*** and ***CASMO-5*** were performed with lattices [

.]

Table 6 and Table 7 show the results of lattice k-infinity calculations performed with both ***CASMO-5*** and ***MCNPX*** at BOC,[

]

Table 6. Comparison of Un-rodded Lattice K-infinity Values at Cold Conditions, BOC

[

]

©2012 Babcock & Wilcox mPower, Inc. All rights reserved.

Table 7. Comparison of Rodded Lattice K-infinity Values at Cold Conditions, BOC

[

]

5.1.1.2 Comparisons at Hot Conditions

[

]

Table 8. Comparison of Un-rodded Lattice K-infinity Values at Hot Conditions, BOC

[

]

©2012 Babcock & Wilcox mPower, Inc. All rights reserved.

Table 9. Comparison of Rodded Lattice K-infinity Values at Hot Conditions, BOC

[

]

5.1.2 ***CASMO-5/MCNPX*** Lattice Depletion Comparisons

Lattice depletions were performed with both ***MCNPX*** and ***CASMO-5*** [

]

[

]

Figure 31. Comparison of *CASMO-5* and *MCNPX* Depletion [ ]

©2012 Babcock & Wilcox mPower, Inc. All rights reserved.

[

]

Figure 32. Comparison of *CASMO-5* and *MCNPX* Depletion [ ]

[

]

Figure 33. Comparison of *CASMO-5* and *MCNPX* Depletion [ ]

©2012 Babcock & Wilcox mPower, Inc. All rights reserved.

5.1.3 Discussion of Results of Lattice Comparisons

The BOC lattice comparisons between ***MCNPX*** and ***CASMO-5*** all show [

]

5.2 Reflector Results

5.2.1 Flux and Current Profiles

Flux and current profiles were generated with both ***MCNPX*** and ***CASMO-5***. [

]

©2012 Babcock & Wilcox mPower, Inc. All rights reserved.

[

]

Figure 34. Homogenized Upper Reflector Detail

[

]

Figure 35. Homogenized Lower Reflector Detail

[

]

Figure 36. Radial Reflector Configuration [ ]

©2012 Babcock & Wilcox mPower, Inc. All rights reserved.

5.2.2 Upper Reflector Comparisons

Figures 37 through 40 show the net current at various locations through the upper reflector regions.

[

]

Figure 37. Net Current Profile in Upper Reflector for Energy Range 1 - 20 MeV

©2012 Babcock & Wilcox mPower, Inc. All rights reserved.

[

]

Figure 38. Net Current Profile in Upper Reflector for Energy Range 5.53 keV - 1 MeV

[

]

Figure 39. Net Current Profile in Upper Reflector for Energy Range 0.625 eV - 5.53 keV

©2012 Babcock & Wilcox mPower, Inc. All rights reserved.

[

]

Figure 40. Net Current Profile in Upper Reflector for Energy Range <0.625 eV

Figures 41 through 44 show the fluxes at various locations through the upper reflector regions. The "a" figures use a linear Y axis to show enhanced detail close to the boundary of the core while the equivalent "b" figures use a logarithmic Y axis to show enhanced detail at greater distances from the core boundary.

©2012 Babcock & Wilcox mPower, Inc. All rights reserved.

[

]

Figure 41a. Flux profile in Upper Reflector for Energy Range 1 - 20 MeV

[

]

Figure 41b. Flux profile in Upper Reflector for Energy Range 1 - 20 MeV (Log Scale)

©2012 Babcock & Wilcox mPower, Inc. All rights reserved.

[

]

Figure 42a. Flux Profile in Upper Reflector for Energy Range 5.53 keV - 1 MeV

[

]

Figure 42b. Flux Profile in Upper Reflector for Energy Range 5.53 keV - 1 MeV (Log Scale)

©2012 Babcock & Wilcox mPower, Inc. All rights reserved.

[

]

Figure 43a. Flux Profile in Upper Reflector for Energy Range 0.625 eV - 5.53 keV

[

]

Figure 43b. Flux Profile in Upper Reflector for Energy Range 0.625 eV - 5.53 keV (Log Scale)

©2012 Babcock & Wilcox mPower, Inc. All rights reserved.

[

]

Figure 44a. Flux Profile in Upper Reflector for Energy Range <0.625 eV

[

]

Figure 44b. Flux Profile in Upper Reflector for Energy Range <0.625 eV (Log Scale)

©2012 Babcock & Wilcox mPower, Inc. All rights reserved.

5.2.3 Lower Reflector Comparisons

Figures 45 through 48 show the net current at various locations through the lower reflector regions.

[

]

Figure 45. Net Current Profile in Lower Reflector for Energy Range 1 - 20 MeV

©2012 Babcock & Wilcox mPower, Inc. All rights reserved.

[

]

Figure 46. Net Current Profile in Lower Reflector for Energy Range 5.53 keV - 1 MeV

[

]

Figure 47. Net Current Profile in Lower Reflector for Energy Range 0.625 eV - 5.53 keV

©2012 Babcock & Wilcox mPower, Inc. All rights reserved.

[

]

Figure 48. Net Current Profile in Lower Reflector for Energy Range <0.625 eV

Figures 49 through 52 show the fluxes at various locations through the lower reflector regions. The "a" figures use a linear Y axis to show enhanced detail close to the boundary of the core while the equivalent "b" figures use a logarithmic Y axis to show enhanced detail at greater distances from the core boundary.

©2012 Babcock & Wilcox mPower, Inc. All rights reserved.

[

]

Figure 49a. Flux profile in Lower Reflector for Energy Range 1 - 20 MeV

[

]

Figure 49b. Flux profile in Lower Reflector for Energy Range 1 - 20 MeV (Log Scale)

©2012 Babcock & Wilcox mPower, Inc. All rights reserved.

[

]

Figure 50a. Flux Profile in Lower Reflector for Energy Range 5.53 keV - 1 MeV

[

]

Figure 50b. Flux Profile in Lower Reflector for Energy Range 5.53 keV - 1 MeV (Log Scale)

©2012 Babcock & Wilcox mPower, Inc. All rights reserved

[

]

Figure 51a. Flux Profile in Lower Reflector for Energy Range 0.625 eV - 5.53 keV

[

]

Figure 51b. Flux Profile in Lower Reflector for Energy Range 0.625 eV - 5.53 keV (Log Scale)

©2012 Babcock & Wilcox mPower, Inc. All rights reserved.

[

]

Figure 52a. Flux Profile in Lower Reflector for Energy Range <0.625 eV

[

]

Figure 52b. Flux Profile in Lower Reflector for Energy Range <0.625 eV (Log Scale)

©2012 Babcock & Wilcox mPower, Inc. All rights reserved.

5.2.4 Radial Reflector Comparisons

Figures 53 through 56 show the net current at various locations through the radial reflector regions.

[

]

Figure 53. Net Current Profile in Radial Reflector for Energy Range 1 - 20 MeV

©2012 Babcock & Wilcox mPower, Inc. All rights reserved.

[

]

Figure 54. Net Current Profile in Radial Reflector for Energy Range 5.53 keV - 1 MeV

[

]

Figure 55. Net Current Profile in Radial Reflector for Energy Range 0.625 eV - 5.53 keV

©2012 Babcock & Wilcox mPower, Inc. All rights reserved.

[

]

Figure 56. Net Current Profile in Radial Reflector for Energy Range <0.625 eV

Figures 57 through 60 show the fluxes at various locations through the lower reflector regions. The "a" figures use a linear Y axis to show enhanced detail close to the boundary of the core while the equivalent "b" figures use a logarithmic Y axis to show enhanced detail at greater distances from the core boundary.

©2012 Babcock & Wilcox mPower, Inc. All rights reserved.

[

]

Figure 57a. Flux profile in Radial Reflector for Energy Range 1 - 20 MeV

[

]

Figure 57b. Flux profile in Radial Reflector for Energy Range 1 - 20 MeV (Log Scale)

©2012 Babcock & Wilcox mPower, Inc. All rights reserved.

[

]

Figure 58a. Flux Profile in Radial Reflector for Energy Range 5.53 keV - 1 MeV

[

]

Figure 58b. Flux Profile in Radial Reflector for Energy Range 5.53 keV - 1 MeV (Log Scale)

©2012 Babcock & Wilcox mPower, Inc. All rights reserved.

[

]

Figure 59a. Flux Profile in Radial Reflector for Energy Range 0.625 eV - 5.53 keV

[

]

Figure 59b. Flux Profile in Radial Reflector for Energy Range 0.625 eV - 5.53 keV (Log Scale)

©2012 Babcock & Wilcox mPower, Inc. All rights reserved.

[

]

Figure 60a. Flux Profile in Radial Reflector for Energy Range <0.625 eV

[

]

Figure 60b. Flux Profile in Radial Reflector for Energy Range <0.625 eV (Log Scale)

©2012 Babcock & Wilcox mPower, Inc. All rights reserved.

5.2.5 Discussion of Results

[

]

5.3 Startup Physics Calculation Comparisons

5.3.1 BOC States

[

] The results of these comparisons are shown in Table 10.

Table 10. Comparison of K-Effective Values at Several BOC Configurations using MCNPX and SIMULATE-3

[

]

Note that, in these comparisons, the differences between the ***MCNPX*** and ***SIMULATE-3*** k-effective values [

]

©2012 Babcock & Wilcox mPower, Inc. All rights reserved.

5.3.2 Moderator and Fuel Temperature Coefficients

Two measurements that are typically performed during the startup of a new reactor system are the moderator temperature coefficient (MTC) and fuel temperature coefficient (represented by the uniform Doppler perturbation (UDP) calculation). The MTC and UDP [

]

The base state from which both coefficients were calculated in ***SIMULATE-3*** was from a k-effective value of [

]

5.3.3 Shutdown Margin

A typical cold shutdown margin analysis was performed to determine the k-effective of the core with the highest worth control rod assembly withdrawn from the core. The target value for the B&W mPower reactor is [

]

5.3.4 Rod Worths

Because rod worths are highly dependent on the conditions and configuration of the core, the position of adjacent rods, and the time in life at which the analysis is performed, the simplest approach of performing the calculation in conjunction with the cold shutdown margin calculations was selected. [

].

©2012 Babcock & Wilcox mPower, Inc. All rights reserved.

[

]

5.4 ***SIMULATE-3/MCNPX*** Core Depletion Comparison

This section compares the results of full core depletion simulation using ***SIMULATE-3*** and an equivalent simulation using ***MCNPX***. Using the methodology described in Section 3.5.2, depletions to [

]

©2012 Babcock & Wilcox mPower, Inc. All rights reserved.

Table 11 shows the details of the depletion steps performed with both codes. The rod groups identified as the [ ] are identified according to the map in Figure 61.

[

]

Figure 61. Quarter Core Control Rod Group Map (Mirror Symmetric)

The resulting k-effective as a function of time for the active depletions steps are shown in Figure 62a. Figure 62b shows the same data, but with a log scale on the burnup axis to emphasize the early time steps. The differences between the k-effective lines are shown in Figure 63a and Figure 63b. Both log scale graphs display the 0.0 GWd/MTU burnup point at 0.001 GWd/MTU, since 0.0 is not a valid point on a log scale. Figure 64a and Figure 64b show the hot excess reactivity curves over the [ ] Figure 65a and Figure 65b show the difference in the hot excess reactivity values between ***MCNPX*** and ***SIMULATE-3***. As with the previous log scale graphs, the 0.0 GWd/MTU burnup points are shown at 0.001 GWd/MTU. Figure 66 through Figure 74 show the critical hot full power assembly axial power, thermal flux, and fast flux profiles at [ ] plotted against axial length in centimeters. Figure 75 through Figure 83 show the same profiles at the same time steps for the ARO configuration.

©2012 Babcock & Wilcox mPower, Inc. All rights reserved.

Table 11. Data for SIMULATE-3 and MCNPX Core Depletion Simulations

[

]

©2012 Babcock & Wilcox mPower, Inc. All rights reserved.

[

]

Figure 62a. K-effective as a Function of Burnup

[

]

Figure 62b. K-effective as a Function of Burnup (Log Scale)

©2012 Babcock & Wilcox mPower, Inc. All rights reserved.

[

]

Figure 63a. Difference in K-effective Values Between *MCNPX* and *SIMULATE-3*

[

]

Figure 63b. Difference in K-effective Values Between *MCNPX* and *SIMULATE-3* (Log Scale)

©2012 Babcock & Wilcox mPower, Inc. All rights reserved.

[

]

Figure 64a. All Rods Out K-effective Comparison

[

]

Figure 64b. All Rods Out K-effective Comparison (Log Scale)

©2012 Babcock & Wilcox mPower, Inc. All rights reserved.

[

]

Figure 65a. Difference in ARO K-effective Values Between MCNPX and SIMULATE-3

[

]

Figure 65b. Difference in ARO K-effective Values Between MCNPX and SIMULATE-3 (Log Scale)

©2012 Babcock & Wilcox mPower, Inc. All rights reserved.

[

]

Figure 66. Assembly Relative Power Fraction Profiles at BOC, Critical Hot Full Power

©2012 Babcock & Wilcox mPower, Inc. All rights reserved.

[

]

Figure 67. Assembly Thermal Flux Profiles at BOC, Critical Hot Full Power

©2012 Babcock & Wilcox mPower, Inc. All rights reserved.

[

]

Figure 68. Assembly Fast Flux Profiles at BOC, Critical Hot Full Power

©2012 Babcock & Wilcox mPower, Inc. All rights reserved.

[

]

Figure 69. Assembly Relative Power Fraction Profiles at [ ]

©2012 Babcock & Wilcox mPower, Inc. All rights reserved.

[

]

Figure 70. Assembly Thermal Flux Profiles at [ ]

©2012 Babcock & Wilcox mPower, Inc. All rights reserved.

[

]

Figure 71. Assembly Fast Flux Profiles at [ ]

©2012 Babcock & Wilcox mPower, Inc. All rights reserved.

[

]

Figure 72. Assembly Relative Power Fraction Profiles at [ ]

©2012 Babcock & Wilcox mPower, Inc. All rights reserved.

[

]

Figure 73. Assembly Thermal Flux Profiles at [ ]

©2012 Babcock & Wilcox mPower, Inc. All rights reserved.

[

]

Figure 74. Assembly Fast Flux Profiles at [ ]

©2012 Babcock & Wilcox mPower, Inc. All rights reserved.

[

]

Figure 75. Assembly Relative Power Fraction Profiles at BOC, All Rods Out Hot Full Power

©2012 Babcock & Wilcox mPower, Inc. All rights reserved.

[

]

Figure 76. Assembly Thermal Flux Profiles at BOC, All Rods Out Hot Full Power

©2012 Babcock & Wilcox mPower, Inc. All rights reserved.

[

]

Figure 77. Assembly Fast Flux Profiles at BOC, All Rods Out Hot Full Power

©2012 Babcock & Wilcox mPower, Inc. All rights reserved.

[

]

Figure 78. Assembly Relative Power Fraction Profiles at [ ] All Rods Out Hot Full Power

©2012 Babcock & Wilcox mPower, Inc. All rights reserved.

[

]

Figure 79. Assembly Thermal Flux Profiles at [ ] All Rods Out Hot Full Power

©2012 Babcock & Wilcox mPower, Inc. All rights reserved.

[

]

Figure 80. Assembly Fast Flux Profiles at [ ] All Rods Out Hot Full Power

©2012 Babcock & Wilcox mPower, Inc. All rights reserved.

[

]

Figure 81. Assembly Relative Power Fraction Profiles at [ ] All Rods Out Hot Full Power

©2012 Babcock & Wilcox mPower, Inc. All rights reserved.

[

]

Figure 82. Assembly Thermal Flux Profiles at [ ] All Rods Out Hot Full Power

©2012 Babcock & Wilcox mPower, Inc. All rights reserved.

[

]

Figure 83. Assembly Fast Flux Profiles at [ ] All Rods Out Hot Full Power

©2012 Babcock & Wilcox mPower, Inc. All rights reserved.

The preceding graphs and figures show that the physics of the core as modeled in ***SIMULATE-3*** are very consistent with the results from ***MCNPX***. There is a clear but [

]

A statistical analysis of the differences of the RPFs between ***MCNPX*** and ***SIMULATE-3*** was performed. The 3-D full core representation of the RPFs in the core was represented by [

] respectively. Figure 84 shows the histograms of the corresponding differences.

[

]

Figure 84. Histogram of Difference Distribution at BOC, [ ] (from left to right)

Figure 85 shows the assembly average and maximum relative power fractions at various times in core burnup. The average difference and standard deviation for each time are shown in the figures. The values show good agreement between ***MCNPX*** and ***SIMULATE-3***.

©2012 Babcock & Wilcox mPower, Inc. All rights reserved.

[

]

Figure 85. Assembly Average and Maximum Relative Power Fractions at BOC, [ ]

©2012 Babcock & Wilcox mPower, Inc. All rights reserved.

6. SUMMARY and CONCLUSIONS

6.1 Results Summary

6.1.1 Lattice Comparisons

Lattice comparisons between ***MCNPX*** and ***CASMO-5*** with and without control rods and at cold and hot conditions were performed and all results showed excellent agreement. The variations in k-infinity are summarized as follows:

[

]

6.1.2 Flux and Current Profiles in Reflector Regions

Both the flux and current values in all the reflectors simulations were in excellent agreement:

[

]

6.1.3 Full Core Physics and Depletions

[

]

©2012 Babcock & Wilcox mPower, Inc. All rights reserved.

6.2 Conclusions

Based on the results of the comparisons performed between the results of the reactor core simulations using the ***CMS*** suite using the design methodology developed by B&W mPower, Inc., and the simulations using the detailed first principles model with ***MCNPX***, the ***CMS*** suite combined with the B&W mPower Methodology is an acceptable design and analysis tool for the mPower reactor core. The neutronic input parameters and the resulting steady state results produced using the ***CMS*** suite that are required for subsequent thermal hydraulic and safety analyses are validated and acceptable for these calculations.

Reference 1 states the following:

> "The eigenvalues and local pin power distributions within a fuel assembly calculated using ***CASMO-5/SIMULATE-3*** were compared to the measured results from the critical experiments to determine the accuracy of the computational methodology. The overall comparisons between calculated and measured data are in very good agreement. The standard deviations between the calculated and measured eigenvalues and pin powers are:

Eigenvalues

- ✓ $\sigma_T = 0.00202$ for the UO_2 Cold, Clean Critical Experiments
- ✓ $\sigma_T = 0.00056$ for the UO_2-Gd_2O_3 Cold, Clean Critical Experiments
- ✓ $\sigma_T = 0.00155$ for the UO_2-PuO_2 Cold, Clean Critical Experiments

Pin Powers

- ✓ $\sigma_T = 0.01615$ for the UO_2 Cold, Clean Critical Experiments
- ✓ $\sigma_T = 0.01736$ for the UO_2-Gd_2O_3 Cold, Clean Critical Experiments
- ✓ $\sigma_T = 0.03361$ for the UO_2-PuO_2 Cold, Clean Critical Experiments

The nuclear computational methodology was also verified by making comparisons between computed and measured critical boron concentrations, local and core-wide power distributions, temperature coefficients, and boron and control rod worths using data from TMI-1 Cycles 1 and 2. With respect to the TMI-1 Cycles 1 and 2 power distributions, 1160 relative power distribution (RPD) data points were used in the comparative analysis of the RPD for Cycles 1 and 2. These data points were obtained from RPD maps of 40 core follow state points. In general, there was very good agreement between predicted and measured cycle critical boron concentrations, temperature coefficients, boron and control rod worths, and relative power distributions and axial power shapes. Specifically, the standard deviations for the relative power distributions for TMI-1 Cycles 1 and 2 are:

©2012 Babcock & Wilcox mPower, Inc. All rights reserved.

- ✓ $\sigma_T = 0.03589$ for TMI-1 Cycle 1
- ✓ $\sigma_T = 0.03326$ for TMI-1 Cycle 2
- ✓ $\sigma_T = 0.03453$ for Combined TMI-1 Cycles 1 and 2

The results from the comparative analysis performed in this Topical Report demonstrate that the ***CASMO-5/SIMULATE-3*** methods and model used for nuclear reactor core calculations can accurately predict criticality conditions for various heterogeneous configurations, local and core-wide power distributions, temperature coefficients, boron and control rod worths, etc. for various core operating and burnup states. The scope of the nuclear methodology qualification analysis was designed to encompass a wide range of geometric and material configurations to adequately represent the core physics embodied by the B&W mPower reactor core design concept."

Based on the results presented in Reference 1 and this Supplement, the ***CMS*** suite and the core design methodology developed by B&W mPower, Inc, are equally applicable to the design of the B&W mPower reactor, as they are for large reactors like TMI-1.

In the early years of reactor design and construction by various vendors, since no measured operating plant data were available, a 7.5% uncertainty on the maximum relative power density in the core and a 5% maximum radial relative power density were considered acceptable at that time. These values were represented in terms of their equivalent Nuclear Reliability Factors (NRF), 1.075 and 1.05.

Based on all of the information presented in Reference 1 and this Supplement Report, B&W mPower, Inc, requests approval to use, in the interim, the same above indicated Nuclear Reliability Factors, until such time as operational data from an actual B&W mPower reactor becomes available. We anticipate that the actual NRFs from measured plant data will be less than the above indicated values, primarily due to the greatly improved accuracy of the intended measurement instrumentation [ ] that will be used in the B&W mPower plant, in addition to the state of the art Nuclear Application Software (NAS) that will provide very accurate and reliable plant measured data.

©2012 Babcock & Wilcox mPower, Inc. All rights reserved.

7. List of Acronyms

Acronym	
2D	Two-dimensional (calculations)
3D	Three-dimensional (calculations)
AIC	Silver-Indium-Cadmium Control Rod Absorber Material
ARI	All Rods In
ARO	All Rods Out
BOC	Beginning of Cycle
BOL	Beginning of Life (zero exposure lattice/core)
BPR	Burnable Poison Rod (integral to fuel lattice, non-integral to fuel pin)
B&W	Babcock & Wilcox
BWR	Boiling Water Reactor
CMS	Core Management System
CR	Control Rod
CRA	Control Rod Assembly
CSDM	Cold Shutdown Margin
EOC	End of Cycle
EOFP	End of Full Power
GWd/MTU	Gigawatt days per metric ton of *initial* uranium
HCRD	Control Rod History (regarding the isotopic effects of depletion while controlled)
HEX, HExR	Hot Excess Reactivity
I-718	Special Metals Corporation "Superalloy" type 718
IFBPR	Integral Fuel Burnable Poison Rod (neutron absorber mixed in fuel pin)
ID	Material (or nuclide) identification number; used in Studsvik codes
LBP	Lumped Burnable Poison (not mixed in fuel pin); same as BPR
LHGR	Linear Heat Generation Rate (pellet heat rate kW/ft)
MOC	Middle of Cycle

©2012 Babcock & Wilcox mPower, Inc. All rights reserved

MWd/MTU	Megawatt days per metric ton of *initial* uranium
MWd/kg	Megawatt days per kilogram of *initial* uranium
MWe	Megawatt – electric power
MWt	Megawatt – thermal power
NRC	Nuclear Regulatory Commission
NRF	Nuclear Reliability Factor
PDE	Power Density
ppm	Parts per Million
PWR	Pressurized Water Reactor
RPF	Relative Power Fraction
SDM	(Strongest Rod Out) Shut-Down Margin
SPND	Self Powered Neutron Detector (rhodium power-range detector)
SRO	Strongest Rod Out
SS, SST	Stainless Steel
TBD	To be determined
TD	Theoretical Density
TFU	Fuel Temperature (for ***CASMO-5*** use)
TMO	Moderator Temperature (for ***CASMO-5*** use)
wt%	Weight Percentage (of an element in a compound or mixture)
Zr-2	Zircaloy-2
Zr-4	Zircaloy-4

©2012 Babcock & Wilcox mPower, Inc. All rights reserved.

8. REFERENCES

1. R003-03-002106, "Core Nuclear Design Codes and Methods Qualification", G. W. Neeley et al., August 31, 2010.
2. LA-CP-11-00438, "***MCNPX***™ User's Manual, Version 2.7.0", D. B. Pelowitz, ed., April 2011.
3. "***CASMO-5/CASMO-5M*** – A Fuel Assembly Burnup Program User's Manual", SSP-07/431, Rev. 3, November 2011.
4. "***SIMULATE-3*** Advanced Three-Dimensional Two-Group Reactor Analysis Code User's Manual", SSP-05/15 Rev. 4, September 2007.
5. "***INTERPIN-4*** User's Manual", SSP-07/435, Rev. 0, October 2007.
6. "***CMS-LINK*** User's Manual", SOA-97/04, Rev. 2, April 1999.
7. "***SIMULATE-3*** Advanced Three Dimensional Two-Group Reactor Analysis Code Methodology Manual", Studsvik/SOA-95/18 Rev. 0, October 1995.
8. LA-UR-02-2607, "***MCNPX***™ User's Manual, Version 2.3.0", L. S. Waters, ed., April 2002.
9. NUREG-800, "Standard Review Plan", Section 4.3 Revision 3, March 2007.
10. "Thermophysical Properties of Matter, Volume 12, Thermal Expansion, Metallic Elements and Alloys", Purdue Research Foundation, IFI/Plenum – New York – Washington, 1975.
11. "Thermophysical Properties of Matter, Volume 13, Thermal Expansion, Nonmetallic Solids", Purdue Research Foundation, IFI/Plenum – New York – Washington, 1975.
12. "Nuclides and Isotopes – Chart of the Nuclides", 16th Edition, Lockheed Martin, Knolls Atomic Power Laboratory, 2002.
13. "***CASMO-5*** A Fuel Assembly Burnup Program Methodology Manual", SSP-08/405 Rev. 0, April 2008.

©2012 Babcock & Wilcox mPower, Inc. All rights reserved.

Appendix A Additional Background Details

A.1 *CMS* Code Suite

The ***CMS*** Code Suite is a collection of nuclear reactor design codes developed and maintained by Studsvik Scandpower. They form the basis of the methodology in the design of the B&W mPower-type Core concept. The suite comprises two primary codes ***CASMO-5/SIMULATE-3*** and two supporting codes ***INTERPIN-4/CMS-LINK.*** ***CASMO-5*** is a multigroup two-dimensional transport theory code used to generate lattice cross sections for ***SIMULATE-3***, which is a three dimensional, two-group, steady-state reactor core simulator used to perform incore fuel management studies, core design calculations, and calculations of reactor safety parameters. ***INTERPIN-4*** calculates the steady-state fuel temperature behavior of UO_2 fuel in light water reactor cores. It is used to provide best estimate fuel temperature data for ***CASMO-5*** and ***SIMULATE-3***. ***CMS-LINK*** is a linking code that processes cross section files produced by ***CASMO-5*** into a binary formatted library that can be used by ***SIMULATE-3***.

A.1.1 ***INTERPIN-4***

INTERPIN-4 calculates the steady-state fuel temperature behavior of UO_2 and MOX fuel operating in light water reactor cores [Reference 5]. It is a simplified version of the full scope fuel performance code ***INTERPIN-FRPS***, specifically modified to meet the fuel temperature input requirements for ***CASMO-5*** and ***SIMULATE-3***. A flow diagram for the calculations performed by ***INTERPIN-4*** is shown below in Figure A - 1 (from Reference 5). Based on the nominal operating conditions for a fuel rod in a LWR core, ***INTERPIN-4*** produces estimates of the average fuel temperature as a function of burnup and linear heat generation rate. The average fuel temperature is used as an input for ***CASMO-5***, while the parameterized temperature data as a function of burnup and power (LHGR) is an input table for ***SIMULATE-3***. ***INTERPIN-4*** also provides other data of interest, including the radial temperature distribution throughout the fuel pellet, fuel-cladding gap sizes, thermal conductance, and cladding oxide layer thickness as a function of power density and exposure, and fission gas release fractions. All of these parameters are considered in the calculated temperature data produced for ***CASMO-5*** and ***SIMULATE-3***. However, the methods used in the calculation of the aforementioned parameters are based on the nominal characteristics of industry standard fuel designs and their associated models for fuel thermal, mechanical, and pellet restructuring effects. Since the fuel type proposed for the mPower reference concept design is standard PWR fuel, the temperature data produced by ***INTERPIN-4*** will be adequate for their intended use in ***CASMO-5*** and ***SIMULATE-3***.

©2012 Babcock & Wilcox mPower, Inc. All rights reserved.

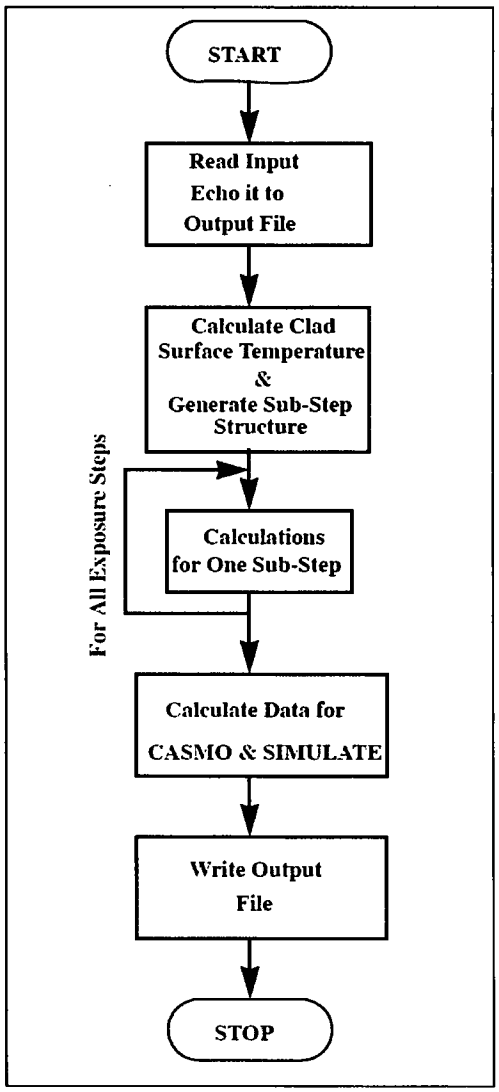

Figure A - 1. *INTERPIN-4* Program Flow

A.1.2 ***CASMO-5***

CASMO-5 is a multi-group two-dimensional transport theory code for burnup calculations on boiling water reactor (BWR) and pressurized water reactor (PWR) assemblies or pin cells [Reference 3]. ***CASMO-5*** is the newest generation of the ***CASMO*** lattice code, and has many improvements over its predecessor, ***CASMO-4***. Some of the high-level physics enhancements that have been added to ***CASMO-5*** include:

1. Quadratic gadolinia depletion model allowing for larger depletion step sizes without compromising accuracy.

©2012 Babcock & Wilcox mPower, Inc. All rights reserved.

2. More exact scattering kernel for resonance upscattering.

3. An energy release model that explicitly computes the isotopic energy yields as lattice compositions evolve, maintaining the physical dependence on fuel exposure, gadolinia, and boron concentrations, MOX composition, and void fractions.

4. Addition of the ENDF/B-VII Cross-Section Library. This extensive update from the previous ***CASMO*** library improves accuracy and enhances resonance treatments including an updated 18-group gamma library for gamma-sensitive in-core detector modeling and gamma energy deposition calculations. Cross-section data is available for over 400 nuclides and materials including more than 200 explicitly defined fission products, 45 heavy nuclides, and an expanded array of detailed depletion chains.

CASMO-5 has been rigorously benchmarked by the code vendor (Studsvik Scandpower) against measured critical experiments, post-irradiation benchmarks, and continuous-energy Monte Carlo calculations, including: (1) B&W Series 1810 and 1484, DIMPLE, and KRITZ-4 criticals; (2) ***MCNP*** (BOL and ***MCODE*** depletions) for pin-cells and whole assemblies; and (3) JAERI nuclide benchmarks. These tests have demonstrated excellent agreement with no significant bias versus the number of gadolinia pins, number of Ag-In-Cd rods, boron concentration, geometry, or presence of reflector/baffle. The overall accuracy of ***CASMO-5*** and its associated ENDF/B-VII neutron data library have been repeatedly validated, ensuring reliably accurate results regardless of core type, fuel type, or operating strategy.

CASMO-5 handles a geometry consisting of cylindrical fuel rods of varying composition in a square pitch array with allowance for fuel rods loaded with gadolinium, erbium, integral fuel burnable absorber (IFBA) pellets, burnable absorber rods (BPR), cluster control rods, incore instrument channels, water gaps, and cruciform control rods in the regions separating fuel assemblies. Reflector/baffle calculations can also be performed with ***CASMO-5***. ***CASMO-5*** incorporates the direct microscopic depletion of burnable absorbers such as gadolinia and erbium into the main calculation and a fully heterogeneous model is used for the two-dimensional transport calculation.

The two-dimensional transport solution methodology used by ***CASMO-5*** is based upon the Method of Characteristics and can be performed in a number of different energy group structures. The macroscopic group cross-sections for ***CASMO-5*** are prepared for the micro-group calculations. The nuclear data library of 586 energy groups covering a range from 0 to 20 MeV are an integral part of the code system and macroscopic cross-sections are directly calculated from the densities, geometries, etc., provided in the user's input.

The effective cross-sections in the resonance energy region for resonance absorbers are calculated using an equivalence theorem that relates tabulated effective resonance integrals for each resonance absorber in each resonance group to the particular heterogeneous problem. The equivalence expression is derived from rational approximations for the fuel self-collision probability. The resonance integrals obtained from the equivalence theorem are used to calculate effective absorption and fission cross-sections. The "shadowing" effect between different pins is taken into account through the use of Dancoff factors that are calculated internally by ***CASMO-5***.

©2012 Babcock & Wilcox mPower, Inc. All rights reserved.

The resonance region, the energy region where data is explicitly shielded in ***CASMO-5***, is defined to lie between 10 eV and 9.118 keV. Absorption above 9.118 keV is assumed to be unshielded. The 1 eV resonance in Pu-240 and other low energy resonances in plutonium and other nuclides are adequately covered by the concentration of thermal groups around these resonances and are consequently excluded from the special resonance treatment.

The cross-sections thus prepared are used in a series of collision probability micro-group calculations to obtain detailed neutron energy spectra in the 586 energy groups used for the energy condensation of the cross-sections. The micro-group calculations are quite fast and are repeated for each type of pin in the assembly, such that individual spectra are obtained for each pin type, e.g., pins containing fuel of different enrichment. To provide micro-group spectra for condensation of an absorber pin cell, a micro-group calculation is performed for the absorber rod surrounded by coolant and a buffer region representing the surrounding fuel pins. The same procedure is used to determine micro-group spectra for water holes within the assembly. The generated cross-section data constitutes the input to the heterogeneous, two-dimensional characteristics based transport calculation, normally performed in 19 or 35 energy groups, which gives the eigenvalue and the associated flux distribution.

Isotopic depletion as a function of burnup is calculated for each fuel pin and for each region containing a burnable absorber. Ten radial rings are typically used for the depletion of gadolinia within a pellet. The burnup calculation is performed using a predictor-corrector approach. For each burnup step, the depletion is calculated twice, first using the spectra at the start of the step, and then after a new spectrum calculation, using the spectra at the end of the step. Average number densities from these two calculations are then used as starting values for the next burnup step.

Reflector data, including data for homogenized baffle/water are accurately generated by a two-dimensional calculation modeling one segment plus the reflector on one side. ***CASMO-5*** contains an automated case matrix capability for generating data suitable for the downstream three-dimensional nodal code, ***SIMULATE-3***. ***CASMO-5*** also contains a module that calculates prompt and delayed gamma sources and solves the 18-group, two-dimensional gamma transport problem such that the gamma detector response may be calculated.

CASMO-5 can accommodate symmetric fuel assemblies using half, quadrant, or octant symmetry as well as fully non-symmetric fuel bundles. Absorber rods or water holes covering 1x1, 2x2, 3x3, or 4x4 pin cell positions are allowed within the assembly. Thermal expansion of dimensions and densities is performed automatically. ***CASMO-5*** employs a simple user oriented input with default values available for many input quantities and nuclear data are automatically read from the library, which is an integral part of the ***CASMO-5*** code package. Input and number densities may be saved on a restart file at each burnup step and used in subsequent calculations.

The ***CASMO-5*** output is designed to be flexible and generates edits for the eigenvalue, the power distribution, reaction rates and few-group parameters for use in core calculations. The output also contains flux discontinuity factors for assembly interfaces and reflector regions. These discontinuity factors are used by ***SIMULATE-3*** in two or multi-group

©2012 Babcock & Wilcox mPower, Inc. All rights reserved.

diffusion theory in order to preserve net currents calculated by the ***CASMO-5*** multigroup transport solution. Figure A - 2 (from Reference 3) summarizes the ***CASMO-5*** program computational flow.

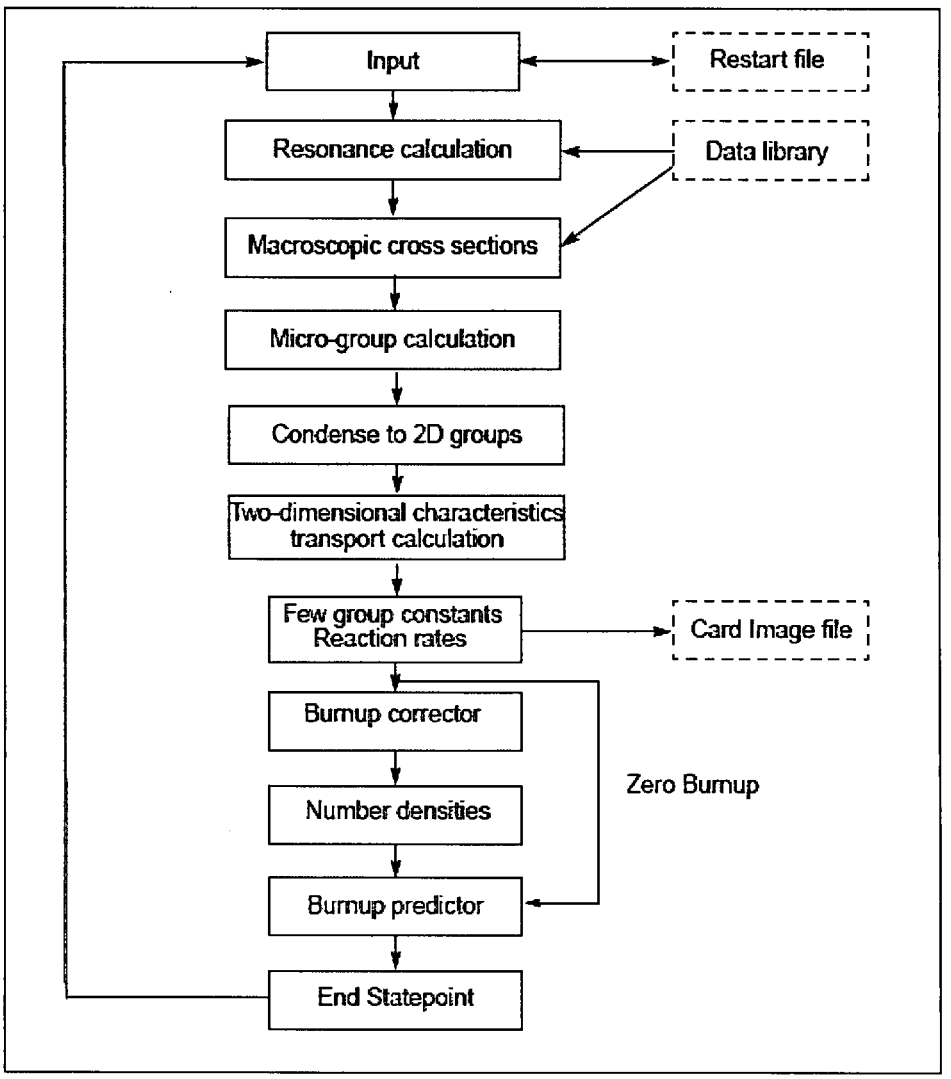

Figure A - 2. *CASMO-5* Program Computational Flow

A.1.3 ***CMS-LINK***

CMS-LINK [Reference 6] is a linking code that processes ***CASMO-5*** Card Image files into a binary formatted nuclear data library for use by ***SIMULATE-3***. The code collects the two-group macroscopic cross-sections, two-group discontinuity factors, fission product data, detector data, pin power reconstruction data, kinetics data, isotopic data, and spontaneous fission data from the ***CASMO-5*** Card Image files and creates a binary library for

©2012 Babcock & Wilcox mPower, Inc. All rights reserved.

SIMULATE-3. ***CMS-LINK*** is capable of processing data for: (1) standard hot and cold PWR segments with and without burnable poison; (2) pulled and reinserted burnable poison for PWR segments; (3) standard cold and hot BWR segments; (4) standard cold and hot PWR and BWR reflector segments; and (5) scoping libraries.

The data functional dependencies (case matrices) that depend on the reactor type are predefined in the code. The library functionalization used for the macroscopic cross-sections is used for the fission product data and discontinuity factors as well. The pin library that includes pin peaking, kinetics, isotopic and detector data is written for each fuel segment by default. The one-dimensional tables of these parameters are determined by the program. The output of the code is a summary of card image file content, segments present in the library both before and after the execution of the code, the case matrix functionalization, and tables of k-infinity values.

A.1.4 ***SIMULATE-3***

SIMULATE-3 is a three-dimensional, two-group, steady-state reactor core simulator that performs incore fuel management studies, core design calculations, and calculation of safety parameters [Reference 3]. ***SIMULATE-3*** employs an advanced nodal expansion method (***QPANDA*** model [Reference 7]) to solve the two-group neutron diffusion theory representation of the reactor core without requiring normalization to fine-mesh calculations or to measured data. ***SIMULATE-3*** provides for thermal-hydraulic feedback, modeling of equilibrium or time-dependent xenon and samarium, and isotopic depletion. In addition, it allows for the generation of pin-by-pin power distributions using a pin power reconstruction technique.

The ***SIMULATE-3*** solution methodology involves subdividing the spatial domain of the reactor into a set of rectangular parallelepiped nodes, with each node typically representing a full assembly or a quarter assembly in the radial plane and a 15-30 cm axial region of an assembly. The three-dimensional diffusion equation is integrated over the volume of each node to obtain the neutron balance equation. Determination of the nodal averaged scalar fluxes requires the intra-nodal flux distributions in both the fast and thermal groups that are derived by integrating the three-dimensional diffusion equation over two of the three directions of a node to obtain a transverse-integrated one-dimensional diffusion equation. Using a fifth-degree polynomial representation for the transverse-integrated flux distribution within a node and a quadratic polynomial representation for the net leakage so that the transverse leakage shape preserves the average transverse leakage in each of the neighboring nodes, an iterative solution to the nodal balance equation is performed until the nodal coupling coefficients and node-averaged fluxes are converged.

The ***SIMULATE-3*** nodal code allows octant-, quadrant-, half-, and full-core geometries. In quarter- and half-core cases, reflective or rotational boundary conditions are permitted on the core interior boundaries. ***SIMULATE-3*** explicitly models the radial and axial reflectors, and conventional albedo conditions are not required at the core periphery. The diffusion equation does, however, require a boundary condition at the outer surface of the reflector. Either zero flux or zero incoming flux boundary conditions can be used, and the sensitivity of the solution to the boundary condition is extremely small if the reflector region is comparable in size to a fuel assembly. ***SIMULATE-3*** allows rotationally symmetric and reflective

©2012 Babcock & Wilcox mPower, Inc. All rights reserved.

boundary conditions. In addition, special studies are permitted with infinite geometry boundary conditions: opposite face periodic, rotationally symmetric, and reflective.

The reactor power, coolant density, and fuel temperature distributions are intimately coupled in ***SIMULATE-3***. The code performs a coupled neutronics/thermal-hydraulics iteration to find these distributions. At any point during the iterative process, the reactor power distribution is considered known, and the coupled problem is reduced temporarily to a problem of determining the coolant density and fuel temperature distributions for a fixed power distribution. The thermal-hydraulic model used in ***SIMULATE-3*** for PWRs is a simple heat balance model that assumes: (1) the coolant inlet flow and temperature distributions are known; (2) the coolant flow is in parallel channels, cross flow is ignored, and the core exit water condition remains subcooled; (3) the power produced by fuel rods within a node is also deposited in the coolant in that node; and (4) the pressure drop across the core is assumed to be negligible, and all water properties are evaluated at a single pressure. These assumptions imply that the coolant enthalpy distribution can be calculated by a simple heat balance of the enthalpy at the inlet of a node, the heat generated within the node, and the enthalpy at the outlet of a node. The node-average density is calculated by evaluating the state properties of water at the average of the node inlet and outlet enthalpies. The average temperature of the fuel pellets in any given node is calculated from a polynomial fit to nodal power density relative to the core averaged power density at 100% of rated power and the moderator temperature. As a result, the fuel temperature coefficients may be different for each fuel segment type in the core.

A.1.5 ***MCNPX*** Code Description

The Monte Carlo N-Particle (eXtended) Transport Code (***MCNPX***) is a general purpose Monte Carlo radiation transport code developed and maintained by Los Alamos National Laboratory [Reference 2]. The current version, ***MCNPX*** 2.7.0, is both the latest public release of the code and the last version of the code that will be released. ***MCNPX*** was developed in 1994 as an extension of ***MCNP4B*** and ***LAHET*** 2.8 in support of the Accelerator Production of Tritium Project. The code was intended to extend the radiation transport capabilities of ***MCNP*** beyond neutrons, photons, and electrons, to all particles and all energies. The project included improvements to the physics models, extension of the cross section libraries for neutron, protons, and photonuclear reactions up to 150 MeV, improvements to the variance reduction and data analysis techniques, incorporating new cross section measurements, benchmark experiments, and deterministic code development, and the addition of a transmutation capability under the ***CINDER90*** project. During that same time, the parent code, ***MCNP***, continued to be maintained and updated by LANL along a separate development path. Many of the transport and model enhancements that were developed for ***MCNP*** were also incorporated into ***MCNPX***. Ultimately, it was decided that the two codes should be merged back together and all of the capabilities of both codes will be combined in the forthcoming release of ***MCNP6***. However, for the purposes of this report, ***MCNPX*** contains all of the features necessary to benchmark the B&W mPower design methodology, specifically the kcode capability to determine the critical eigenvalue in a reactor system, detailed ENDF/B-VII cross sections for all relevant radionuclides, and the isotope generation and depletion capability encompassed in the ***CINDER90*** module. A detailed discussion of the underlying interaction physics contained in ***MCNPX*** can be found

©2012 Babcock & Wilcox mPower, Inc. All rights reserved.

in Chapters 4 and 5 of the ***MCNPX*** User's Manual, Version 2.3.0, released in 2002 [Reference 8].

MCNPX was released by LANL through the Radiation Safety Information and Computational Center (RSICC) in July 2011. While models had already been developed and tested using the previously released ***MCNPX*** 2.6.0, the burn capability in the ***CINDER90*** subroutine of that version of the code was considered a "beta" capability. Through successive interim beta releases from LANL, the depletion capability matured and was finalized in the last release.

Unlike the ***CMS*** code suite, ***MCNPX*** does not have a reactor simulator module. The area where ***MCNPX*** excels is in the detailed calculation of the transport of radiation through Monte Carlo methods using explicit energy-dependent microscopic cross sections. There is no capability in ***MCNPX*** to calculate the effect of the thermal feedback of the moderator on the core as a whole for any given operating point, and using ***MCNPX*** in an actual design mode is not possible with current computational technology. However, by incorporating consistent design features (e.g., thermal expansion and material compositions) from ***CASMO-5*** and copying a limited set of the nodal characteristics (e.g., fuel, clad, and moderator temperatures and densities) from ***SIMULATE-3*** for a given statepoint, ***MCNPX*** can be used to mimic the operation of ***SIMULATE-3*** with all the detailed physics and cross sections of a Monte Carlo transport code. Thus, it becomes possible to use ***MCNPX*** to "follow" a core designed using ***SIMULATE-3*** and validate the underlying physics of the results.

A.1.6 Model Inputs and Considerations

Preparing the inputs for the various code packages requires consideration of the endpoint use of the information being generated by the software and any limitations inherent in the respective packages. Detailed in the subsequent sections are the general input file parameters and application-specific considerations that were made for each software package used in these analyses. Some are directly relevant to and used in the reference core design. Others are modifications that were made to accommodate limitations in the modeling capabilities or the ability of one code to produce results that are directly comparable to the output from another code.

A.1.7 ***INTERPIN-4***

The ***INTERPIN-4*** code, as indicated above, provides a set of temperature data for both ***CASMO-5*** and ***SIMULATE-3***. Since there are three different bundle types, characterized by the number of BPRs in the assembly [ ] ***INTERPIN-4*** runs are required to fully characterize the temperature parameters used in the design of the core.

Table A - 1 shows the required parameters for the input files for the three ***INTERPIN-4*** runs. All but one of the input parameters are identical, regardless of the number of BPRs. The only value that changes with the number of BPRs is the average linear heat generation rate.

©2012 Babcock & Wilcox mPower, Inc. All rights reserved.

Table A - 1. *INTERPIN-4* Input Parameters

[

]

The resulting respective average fuel and moderator temperatures in an assembly with [

]

The assembly-dependent average fuel and moderator temperature values are used as inputs for ***CASMO-5*** for the primary, at power, depletion case when generating the lattice cross sections. The tabular values for temperature as a function of burnup and power level are used as inputs for ***SIMULATE-3***. They are also used in the calculation of the initial thermal expansion of the various materials (fuel, cladding, BPRs, etc.) and in the determination of the material cross sections.

©2012 Babcock & Wilcox mPower, Inc. All rights reserved.

A.1.8 ***CASMO-5***

The lattice physics code, ***CASMO-5***, is the fundamental basis upon which the core design is constructed. It provides the cross section data for each lattice at all points in the life of the reactor core. The basic parameters for a typical input file include the average fuel and moderator temperatures (from the relevant ***INTERPIN-4*** run), the pressure at the core midplane, the average core power density, and the basic lattice structure, including the number of pins along one side of an assembly and the pin and assembly pitch values. Once the basic characteristics of the core and assembly have been specified, all of the pin geometry specifications and the comprising materials are defined, including the locations of the fuel and non-fuel pins, the control rods, and the instrument tube.

The primary depletion calculation is run at the specified average moderator and fuel temperature and pressure conditions. Additional depletion cases are run with different fuel and moderator temperatures and also with the primary control rod inserted. Branch cases are defined from those baseline depletions that are used to functionalize the relationship between the conditions of those baseline depletions and various parameters that may be indicative of relatively instantaneous changes in certain situations (e.g., shutdown to cold conditions). The functionalization relates the primary operating parameters, including moderator temperature, fuel temperature, pressure, etc., and the resulting effects on the energy dependent flux distribution in the lattice, the accompanying depletion of the fuel and burnable poisons, and the buildup of fission products. Though the case matrix for most reactors includes boron history depletion and boron branch cases, no such options were included for the mPower reference design.

As part of the work performed for this report, a depletion calculation was run using ***CASMO-5*** for each of the primary lattices in the B&W mPower reference design. These lattice runs were compared against equivalent lattice depletion runs in ***MCNPX***. For the comparative depletion calculations with ***MCNPX***, the only change to the ***CASMO-5*** input files that was necessary to accommodate comparison with ***MCNPX*** runs was the [ ] ***CASMO-5*** uses a method in which the cumulative mass of all the spacers is homogenized throughout the coolant in the assembly and then, when the core is constructed in ***SIMULATE-3***, each spacer is "reconstituted" in its individual solid form. Given the limited effect of including the spacer in the lattice calculations, the more straightforward comparison of the lattices [ ] was performed. The full core ***MCNPX*** models include the actual spacers for direct comparison with ***SIMULATE-3***.

In addition to the basic lattice calculations, ***CASMO-5*** is also used to perform reflector calculations to characterize the neutron leakage into and out of the core and account for the thermalization of neutrons outside the core that may ultimately return and cause additional fissions.

A.1.9 ***SIMULATE-3***

The reference core design is constructed in the ***SIMULATE-3*** input file. The 586-group cross section data and all the heterogeneous structure of the assembly is reduced to a two-group, homogenized nodal representation. The homogenized nodes are stacked and

©2012 Babcock & Wilcox mPower, Inc. All rights reserved.

organized into the construct that represents the full core design. The primary depletions and all the branch cases are fully functionalized so that the operational characteristics of the core design can be fully examined. ***SIMULATE-3*** uses some simplifications which should be taken into account when comparing the operation of the model against an actual reactor. One of the first simplifications is reflected in the thermal hydraulic model used for the coolant in the core. The flow is assumed to be one-dimensional without cross flow, such that all power produced in a node is deposited in that node and that power (enthalpy) stays in that channel. Further, the pressure drop through the core is ignored and the properties of the coolant are evaluated at the pressure specified in the input file. The bypass flow through the guide and instrument tube is not explicitly modeled and the flow and temperature at the inlet to each assembly are assumed to be uniform. The assembly exit conditions are always assumed to be sub-cooled when modeling a PWR, even if the temperature and pressure would indicate otherwise (warnings are generated if this is the case). The end user must be aware of this issue and evaluate whether or not this assumption is valid for the design under consideration. [

.]

A second approximation is that the control rod material "disappears" as it is withdrawn from the core. The withdrawn portion of the control rod cluster disappears at the interface between the core and the upper axial reflector in a PWR, i.e., there is no representation of the material in the control rods in the homogenized reflector layers above the core. The ***SIMULATE-3*** methodology does not recommend the homogenization of typical control rod materials in a reflector, as it would overestimate the absorptive properties of that reflector.

A.1.10 ***MCNPX*** Model Description

The ***MCNPX*** model for the mPower reference design has been under development from the very beginning of the project and has evolved to a full-featured model that contains all the details necessary to perform a wide range of calculations. The model is maintained in a spreadsheet format that minimizes the required manual input such that there is little opportunity for human error. [

]

©2012 Babcock & Wilcox mPower, Inc. All rights reserved.

[

]

Figure A - 3. Axial Cross Section View of *SIMULATE-3*-Equivalent *MCNPX* Model

©2012 Babcock & Wilcox mPower, Inc. All rights reserved.

[

]

Figure A - 4. Radial Cross Section View of *SIMULATE-3*-Equivalent *MCNPX* Model

A.2 Regulatory Considerations

The process by which new reactor core designs are certified typically relies on similarities between the new design and prior designs and software that has been sufficiently validated to those prior designs. Reference 9 states, "For a normal review, many areas related to core power distribution will have been examined in generic reviews of reactors with generally similar core characteristics and instrument systems." Thus, an applicant for a design certification will generally demonstrate that the relevant code base adequately models the previous design and,

©2012 Babcock & Wilcox mPower, Inc. All rights reserved.

because of the similarities between the old design and the new design, is thus equally applicable to the proposed new design. The challenge with the B&W mPower Reference Core concept lies in the fact that there are no reactors of similar configuration, size, and power, from which operational data is available to validate the Studsvik ***CMS*** suite methodology. However, by benchmarking the ***CMS*** suite against a first-principles Monte Carlo code like ***MCNPX***, a reasonable degree of assurance can be obtained that the code suite is modeling the physics of the design accurately, and is thus valid for the design of a small core like the B&W mPower reactor.

©2012 Babcock & Wilcox mPower, Inc. All rights reserved.

Appendix B Additional Methodology Details

B.1 Lattice Construction

B.1.1 ***MCNPX*** Lattice Construction

The input files for the ***MCNPX*** lattice runs were all constructed in the same manner as ***CASMO-5***. [

]

©2012 Babcock & Wilcox mPower, Inc. All rights reserved.

[

]

B.1.2 ***MCNPX*** Lattice Depletion Simulations

The lattice depletion in ***MCNPX*** works in tandem with the kcode calculations performed for each depletion step. [

]

©2012 Babcock & Wilcox mPower, Inc. All rights reserved.

B.2 Design Specifications

The sections below describe in specific detail the design inputs for the lattices used in the B&W mPower core reference design, including the geometric size and spacing of all the components, the materials, and any other relevant parameters.

B.2.1 Mechanical Design

A complete set of ***CMS*** inputs has relatively few mechanical design inputs since these codes are (for the most part) concerned with LWR core power distribution and fuel depletion calculations. With the exception of reflector calculations performed with ***CASMO-5*** for use as boundary conditions in ***SIMULATE-3***, these codes are concerned only with the fueled portion of the core (fuel assembly/bundle). Only the mechanical input necessary for specification of the B&W mPower lattices that make up the fuel assembly are discussed here.

Note that fuel pins may have [

]

©2012 Babcock & Wilcox mPower, Inc. All rights reserved.

Table B - 1. B&W mPower *CASMO-5* Control Rod Assembly Specification

[

]

Table B - 2. Fuel Assembly Mechanical Design Inputs

[

]

©2012 Babcock & Wilcox mPower, Inc. All rights reserved.

Table B - 3. Neutronic Design Parameters

[

]

©2012 Babcock & Wilcox mPower, Inc. All rights reserved.

Table B - 3. Neutronic Design Parameters (cntd.)

[

]

©2012 Babcock & Wilcox mPower, Inc. All rights reserved.

Table B - 3. Neutronic Design Parameters (cntd.)

[

]

B.2.2 Material Properties

This section details the materials and their properties as used in the ***CASMO-5*** model inputs. All material densities are based on room temperature conditions, 293 K (68 °F).

A. Assumptions common to ***CMS*** codes input files

[

]

©2012 Babcock & Wilcox mPower, Inc. All rights reserved.

B. Assumptions made in the ***CASMO-5*** input file

1) All values specified in the ***CASMO-5*** input file use **metric units**:

Material densities:	gram/cm^3
Temperatures:	K (Kelvin)
Dimensions:	cm
Pressure:	bar (1 bar = 14.504 psi)
Burnup (Exposure):	MWd/kg (= GWd/metric ton)

[

]

©2012 Babcock & Wilcox mPower, Inc. All rights reserved.

[

]

©2012 Babcock & Wilcox mPower, Inc. All rights reserved.

[

]

©2012 Babcock & Wilcox mPower, Inc. All rights reserved.

[

]

©2012 Babcock & Wilcox mPower, Inc. All rights reserved.

[

]

©2012 Babcock & Wilcox mPower, Inc. All rights reserved.

[

]

©2012 Babcock & Wilcox mPower, Inc. All rights reserved.

[

]

©2012 Babcock & Wilcox mPower, Inc. All rights reserved.

B.2.3 Operating Parameters

The global operating characteristics of the B&W mPower reference design as of January 11, 2012, are detailed below in Table B - 4. There are no changes being contemplated (as of the writing of this report) in the size and power output of the reactor. However, as additional analyses are performed, particularly the thermal hydraulic modeling, changes to the flow rate, inlet and outlet temperatures, and the pressure have since been determined to be necessary. All such changes are anticipated to be minor and should not impact the conclusions of the analyses contained herein.

Table B - 4. B&W mPower Operating Characteristics

Parameter	**Value**
Core data	
Number of fuel assemblies in the core	69
Number of control rod assemblies in the core	69
Rated thermal power (MWt)	530
Electric output (MWe)	180
Rated core flow (Mlb/hr)	30.0
Core inlet temperature (K/°F)	569.0 / 564.53
Core outlet temperature (K/°F)	593.15 / 608.0
Reactor dome pressure (psia)	2050

B.2.4 Lattice Input Specifications

All of the previously detailed information is synthesized into a relatively simple input file for the ***CASMO-5*** lattice calculations. The first two lines of the input file identify the title of the run and the name of the lattice (used in ***SIMULATE-3***). A sample of these input specifications is shown below in Figure B - 1.

[

]

Figure B - 1. *CASMO-5* Title and Name Card Input

The next few lines of the input file describe the [

]

©2012 Babcock & Wilcox mPower, Inc. All rights reserved.

[

]

Figure B - 2. *CASMO-5* Global Operating Parameters

[

]

[

]

Figure B - 3. *CASMO-5* Material Specifications

The next section of the input file contains [

]

©2012 Babcock & Wilcox mPower, Inc. All rights reserved.

[

]

Figure B - 4. *CASMO-5* Pin Geometry Specifications

[

]

©2012 Babcock & Wilcox mPower, Inc. All rights reserved.

[

]

Figure B - 5. *CASMO-5* Fuel and Pin Array Specifications

[

]

[

]

Figure B - 6. Closing *CASMO-5* Input Cards

©2012 Babcock & Wilcox mPower, Inc. All rights reserved.

B.2.5 Cross Section and Energy Considerations

B.2.5.1 Resonance Upscattering

Reference 13 states that ***CASMO-5*** includes a new resonance upscatter model that is intended to address the difference between the asymptotic scattering kernel in the resonance range implemented in the ***NJOY*** series of codes and the exact scattering kernel. The asymptotic scattering kernel does not allow for the upscattering of neutrons in the vicinity of scattering resonances. The effect on the neutron spectrum and the resonance integrals can be significant, particularly at low energies (e.g., the low energy resonances of U-238). With this correction, Doppler coefficients in ***CASMO-5*** are expected to be about 10 percent more negative for a typical LWR calculation. Reference 13 also states that, when comparing ***CASMO-5*** to a Monte Carlo code (e.g., ***MCNP5*** [or ***MCNPX***]) that only has an asymptotic scattering kernel, the resonance upscattering correction should be turned off. [

]

B.2.5.2 Energy Group Structure

The energy group structure for all calculations performed with ***CASMO-5*** begins with 586 groups and is gradually reduced down to the default two group cross sections that are used in ***SIMULATE-3***. However, it is also possible to perform isolated ***CASMO-5*** calculations in different energy group structures, up to a maximum of 586 groups. Given that, regardless of the number of groups used for the 2D transport calculation, the
[

]

B.2.5.3 Resonance Self-Shielding

Resonance self-shielding is implicitly taken into account in lattice calculations performed with ***MCNPX*** due to the continuous nature of the material cross sections and the use of the Monte Carlo method. ***CASMO-5***, because it reduces the material cross sections to 586 groups does include corrections to the calculated cross sections for resonance self-shielding. [

]

©2012 Babcock & Wilcox mPower, Inc. All rights reserved.

B.2.5.4 Dancoff Factors

The Dancoff correction to the effective resonance absorption cross sections is derived based on the position of the particular fuel pin in the lattice and the geometric and materials characteristics of the lattice. As with the correction for resonance self-shielding, this correction is implicit in Monte Carlo calculations performed with ***MCNPX***. For ***CASMO-5***, the Method of Characteristics requires that the cross sections be adjusted based on the calculated Dancoff factors. The Dancoff factors in ***CASMO-5*** are calculated by assuming the infinite lattice Dancoff factor is equal to that calculated for the surrounding eight fuel pins. [

]

B.2.6 Reflector Calculations

B.2.6.1 Reflector Calculational Methodology

B.2.6.1.1 Homogenized Reflector Description

Reference 5, as well as supplementary Studsvik training materials, state that the reflector slab material specification should use 'HOx' cards (Homogenization of composition), which may be composed of various default compositions (CRS, BOX, etc.) or user specified 'MIx' cards. [

]

B.2.6.1.2 Upper Reflector

The upper reflector was divided [

]

©2012 Babcock & Wilcox mPower, Inc. All rights reserved.

[

]

©2012 Babcock & Wilcox mPower, Inc. All rights reserved.

[

]

[

]

Figure B - 7. *CASMO-5* Input Card Image For Homogenized Upper Reflector

B.2.6.1.3 Lower Reflector

The lower reflector [

]

©2012 Babcock & Wilcox mPower, Inc. All rights reserved.

[

]

©2012 Babcock & Wilcox mPower, Inc. All rights reserved.

[

]

Figure B - 8. *CASMO-5* Input Card Image For Homogenized Lower Reflector

B.2.6.1.4 Radial Reflector

The radial reflector [

]

©2012 Babcock & Wilcox mPower, Inc. All rights reserved.

Appendix C Additional Details of the *SIMULATE-3* Reference Core Operating Cycle

C.1 *SIMULATE-3* REFERENCE CORE OPERATING CYCLE

This report presents the methodology and the results of the 3D core design analyses performed by B&W mPower for the once-through four-year fuel cycle. This core design concept utilizes a number of different lattice designs, with varying burnable poison content and pellet enrichment, and [ ] to meet specific design requirements (energy output, cycle length, power peaking etc).

The scope of this calculation includes:

[

]

C.1.1 Control Rod Sequences

[

]

©2012 Babcock & Wilcox mPower, Inc. All rights reserved.

[

]

Figure C - 1. The [ ] Used in the mPower Cycle Management

[

]

©2012 Babcock & Wilcox mPower, Inc. All rights reserved.

[

]

Figure C - 2. The [ ] Used in the mPower Cycle Management

C.1.2 Control Rod Assembly Layout

Several studies have been performed to determine the optimal control rod assembly configuration that meets the design objective of 3% Δk/k cold shutdown margin. The studies concluded that the standard Ag-In-Cd (AIC) alloy, with a nominal composition of 80 wt% Ag, 15 wt% In and 5 wt% Cd, is suitable for use as the control rod absorber material in the mPower reactor core.

All 69 fuel assemblies in the mPower reactor core are [

]

©2012 Babcock & Wilcox mPower, Inc. All rights reserved.

[

]

C.1.3 Cycle Management (Control Rod Patterns)

This section summarizes the control rod sequences (see Figure C - 3) used from BOC to EOC to control the excess reactivity of the core and to shape the axial and radial power and exposure distribution.[

]

©2012 Babcock & Wilcox mPower, Inc. All rights reserved.

[

]

Figure C - 3. Summary of Control Rod Patterns Used from BOC to EOC

[

]

©2012 Babcock & Wilcox mPower, Inc. All rights reserved.

[

]

Figure C - 3. Summary of Control Rod Patterns used from BOC to EOC (cntd.)

©2012 Babcock & Wilcox mPower, Inc. All rights reserved.

[

]

Figure C - 3. Summary of Control Rod Patterns used from BOC to EOC (cntd.)

©2012 Babcock & Wilcox mPower, Inc. All rights reserved.

[

]

Figure C - 3. Summary of Control Rod Patterns used from BOC to EOC (cntd.)

©2012 Babcock & Wilcox mPower, Inc. All rights reserved.

[

]

Figure C - 3. Summary of Control Rod Patterns used from BOC to EOC (cntd.)

©2012 Babcock & Wilcox mPower, Inc. All rights reserved.

[

]

Figure C - 3. Summary of Control Rod Patterns used from BOC to EOC (cntd.)

The end-of-full-power (EOFP) occurs at [

]

©2012 Babcock & Wilcox mPower, Inc. All rights reserved.

[

]

Figure C - 3. Summary of Control Rod Patterns used from BOC to EOC (cntd.)

©2012 Babcock & Wilcox mPower, Inc. All rights reserved.

C.1.4 Core Axial Offset

Axial offset is defined as the percent difference between the power generated in the upper and the lower halves of the core:

$$\text{Axial Offset} = (Pt - Pb) / (Pt + Pb) \times 100,$$

where Pt and Pb are the integrated powers (sum of nodal powers, as calculated in ***SIMULATE-3***) in the top and bottom halves of the core, respectively.

SIMULATE-3 lists the axial offset values as A-O = (Pt – Pb) / (Pt + Pb), as shown in Figure C - 4.

[

]

Figure C - 4. Power Axial Offset versus Cycle Exposure

©2012 Babcock & Wilcox mPower, Inc. All rights reserved.

C.1.5 Nodal Peaking

Nodal peaking values, as shown in Figure C - 5, represent the peak relative power density at a given exposure. [

]

[

]

Figure C - 5. Nodal Peaking versus Cycle Exposure

©2012 Babcock & Wilcox mPower, Inc. All rights reserved.

C.1.6 Cycle Cold Shutdown Margin

The shutdown margin (SDM) is defined as the amount of reactivity, expressed in %Δk/k, by which the reactor is subcritical with the analytically determined maximum worth control rod assembly assumed stuck in the fully withdrawn position and all other assemblies fully inserted. The *cold* shutdown margin (CSDM), as shown in Figure C - 6, is the level of core subcriticality at 68 °F, atmospheric pressure, and xenon-free conditions (the three parameters that define the "cold" state) with the strongest CRA out. CSDM is calculated with ***SIMULATE-3*** by running 1-rod-out cases, at cold conditions, restarting from the desired statepoints (exposures) in the nominal cycle run. The CSDM provides useful information during the startup after an extended period of shutdown.

[

]

Figure C - 6. Cold Shutdown Margin versus Cycle Exposure

CSDM is highly dependent on the local conditions surrounding the CRA that is assumed to be fully withdrawn. Therefore, CSDM is usually loading pattern dependent.

©2012 Babcock & Wilcox mPower, Inc. All rights reserved.

C.1.7 Cycle Hot Excess Reactivity

The hot excess reactivity (HExR), as shown in Figure C - 7, is the amount of reactivity that must be controlled at normal full power operating conditions using control rods. The higher the hot excess reactivity, the greater the control rod density needed to maintain the reactor at the full power critical state. Too much HExR is disadvantageous, since it would require high control rod densities to control the reactivity. Too little HExR is also undesirable, because it may leave the core with limited capability to overcome xenon transients during power maneuvers. In any case, HExR needs to be greater than 1 in order to maintain a 100% power level (HExR< 1 during coastdown).

Hot excess reactivity is defined as the amount of reactivity, expressed in %Δk/k, by which the reactor would exceed criticality if all CRAs were withdrawn at rated conditions. HExR is calculated with ***SIMULATE-3*** by running ARO cases, at rated conditions, restarting from the desired statepoints (exposures) in the nominal cycle run. Unlike the cold shutdown margin, hot excess reactivity is a core-wide phenomenon.

[

]

Figure C - 7. Hot Excess Reactivity versus Cycle Exposure

©2012 Babcock & Wilcox mPower, Inc. All rights reserved.

C.1.8 Control Rod Movement

Control rod movement, as shown in Figure C - 8, is calculated as centimeters of control rod length inserted (+) or withdrawn (–) in a day and is determined based on initial and final control rod position during a control sequence (or sub-sequence) and assuming continuous adjustment of the "floaters".

[

]

Figure C - 8. Control Rod Movement versus Cycle Exposure

©2012 Babcock & Wilcox mPower, Inc. All rights reserved.

C.1.9 Bundle Power Profile at EOFP

[

]

Figure C - 9. End of Full Power [ ] Axial Power Profile

[

]

©2012 Babcock & Wilcox mPower, Inc. All rights reserved.

C.1.10 Bundle Exposure Profile at EOFP

[

]

Figure C - 10. End of Full Power [ ] Exposure Profile

[

]

©2012 Babcock & Wilcox mPower, Inc. All rights reserved.

Appendix D Additional Details of Results, Comparison, and Analysis

D.1 Lattice Results

The following are additional plots of lattice depletion comparisons using ***CASMO-5*** and ***MCNPX***.

[

]

Figure D - 1. Comparison of *CASMO-5* and *MCNPX* Depletion for [ ]

©2012 Babcock & Wilcox mPower, Inc. All rights reserved.

[

]

Figure D - 2. Comparison of *CASMO-5* and *MCNPX* Depletion [ ]

[

]

Figure D - 3. Comparison of *CASMO-5* and *MCNPX* Depletion [ ]

©2012 Babcock & Wilcox mPower, Inc. All rights reserved.

[

]

Figure D - 4. Comparison of *CASMO-5* and *MCNPX* Depletion [ ]

[

]

Figure D - 5. Comparison of *CASMO-5* and *MCNPX* Depletion [ ]

©2012 Babcock & Wilcox mPower, Inc. All rights reserved.

[

]

Figure D - 6. Comparison of *CASMO-5* and *MCNPX* Depletion [ ]

[

]

Figure D - 7. Comparison of *CASMO-5* and *MCNPX* Depletion[ ]

©2012 Babcock & Wilcox mPower, Inc. All rights reserved.

[

]

Figure D - 8. Comparison of *CASMO-5* and *MCNPX* Depletion[ ]

©2012 Babcock & Wilcox mPower, Inc. All rights reserved.